Author response to the comments during the open discussion phase of "Evaluation of polar stratospheric clouds in the global chemistry-climate model SOCOLv3.1 by comparison with CALIPSO spaceborne lidar measurements"

We would like to thank the two referees as well as Yunqian Zhu and Astrid Kerkweg for their helpful feedback and comments. We appreciate the suggestions, which help to improve our manuscript. We have taken all comments into account and, based on the suggestions, we have significantly extended our model simulations and analyses, as well as the discussion section. The major changes to our manuscript, as suggested by the reviewer, are:

- Additional model simulations and analyses for the Antarctic winters 2006 and 2010, which represent years with above- and below-average PSC occurrence.
- Additional sensitivity simulations to investigate the impact of the model's cold bias on PSC formation: temperature for PSC formation increased by 3K.
- Extended discussion on further influencing factors for PSC formation like model resolution or temperature biases as well as of previous studies.

The detailed answeres to all four comments, as we uploaded them in the final response phase, are given below. These answeres are followed by a marked-up manuscript version, highlighting all textual changes.

Author response to comments of Referee 1

We thank the referee for taking the time to read the manuscript and for the helpful feedback. Although we think that many most of the points raised are already described in the manuscript, it became clear that some clarification is necessary. In response to Referee 1, along with other revisions in response to Referee 2, we extended the description of our PSC scheme (Sect. 2.1) and of our evaluation approach (Sect. 2.4). We hope that our answers and revisions help to clarify the description. We present our responses below, with reviewer comments in blue and author responses in black.

The authors present an interesting study of comparison of the model outputs of the SOCOL model with observations by the satellite-borne lidar CALIOP. The approach is to test if a CCM without a detailed microphysical model for the formation of PSCs can be used to calculate PSCs in the polar regions. The advantage of such an approach is the reduced time for calculations wrt more sophisticated models including microphysical schemes. To demonstrate the merits and deficits of such an approach the model output is processed to obtain optical parameters which allow PSC classification similar to that used by CALIOP. The authors compare the optical constants measured by CALIOP with those obtained from the SOCOL model. How are these optical parameters obtained? The authors state "From the simulated SADs and the assumed microphysical parameters, we calculate the number density and/or radius for each particle type.".

The idea of our study is to evaluate the PSCs simulated by SOCOLv3.1 with the help of backscatter measurements by CALIOP onboard the CALIPSO satellite. For that purpose, we converted the simulated PSCs quantities, namely the SAD of STS, NAT and ice, into a size distribution and calculated the optical signal CALIPSO would measure. This is described in Sect. 2.4.

The general procedure is the following: In SOCOL, NAT and water ice are calculated as soon as the partial pressures of HNO3 and water vapor, respectively, exceed supersaturation. From the excess HNO3 and H2O, the surface area density of NAT and water ice is calculated. Herein we assume for NAT a fixed radius and a maximum number density. The latter assumption prevents that all excess HNO3 goes into NAT particles at the expense of STS formation. This accounts for the fact that NAT and STS clouds are mostly observed simultaneously (e.g. Pitts et al., 2011). Conversely, for water ice we assume a fixed number density and calculate the radius from the total ice volume.

The rationale behind the different treatment of NAT and water ice in the model is the following: For water ice, the time to reach equilibrium between the gas- and particulate phase is very short. That means that, once ice has formed, the ice number density stays quite constant and further cooling leads rather to particle growth than to additional nucleation. In the case of NAT, however, the equilibrium between the gas and particulate phase is hardly reached, as shown by observations (Fahey et al., 2001), and additional particles can nucleate upon further cooling. Therefore, we do not fix the NAT number density, but the radius, which has been optimized to match observed sedimentation/denitrification. We are aware that this bulk parameterization is a simplification of the real world, but it helps keeping computational effort low. To various extents, this is done in most CCMs. Thus, the strongest point of the present analysis is the comparison with the state-of-the-art satellite data.

The basis for STS droplets are binary H2O-H2SO4 aerosol particles, whose distribution is prescribed from a monthly mean observational data record, mainly based on SAGE-observations. The data record provides SAD, volume density, mean radius and H2SO4 mass of the binary aerosol. STS droplets form in the model when gas-phase HNO3 and H2O is taken up by the binary aerosols, following the expression by Carslaw et al. (1995). The uptake of HNO3 and H2O leads to a change in aerosol mass, from which a growth factor of the binary aerosol and therefore the radius of the ternary aerosol can be calculated.

For all three PSC type we outputted the individual surface area density for each model grid point. For the present study we used a 12 hourly output frequency.
To mimic the satellite measurements we proceded as follows: From the outputted SADs of the three PSC types and the above mentioned assumptions on NAT radius and water ice number density as well as with the STS-radius resulting from the above mentioned growth-factor for ternary aerosols, we calculate the missing parameter, i.e. the number density or radius. These quantities are then used in Mie and T-matrix scattering codes (Mishchenko et al., 1996) to compute optical parameters of the simulated PSCs, i.e. R532, δ_aerosol and β⊥. As shapes we assume ellipsoids with an aspect ratio of 0.9 (diameter-to-length ratio) for NAT and ice. STS are liquid particles and therefore assumed to be spherical with a depolarization ratio δ_aerosol = 0.

They also state that the radius of the NAT and STS particles is fixed (5 micron for NAT but we don't know for STS), and that ice has a variable radius, but we don't know how this is obtained. ("The variable radius of ice particles results in a variable $\delta_{aerosol}$ value."). Since the conversion of SAD to particle size distribution and number density has an important impact on the results, the authors should dedicate a paragraph on how this is done.
As mentioned above only the radius of the NAT particles is fixed, not the radius of STS-particles. We noticed that our formulation in the manuscript was indeed very misleading and rephrased the sentence "~~STS and NAT, due to their spherical shape and fixed radius, appear at constant δaerosol-values of 0 and 0.167, respectively.~~" to "STS (due to their spherical shape) and NAT (due to the assumed fixed radius) appear at constant δ_aerosol-values of 0 and 0.167, respectively."

Why don't they use a size distribution for all particles, instead of applying observational uncertainties to the results of the Mie calculations? This is of course an artificial way to obtain some scattering of the results but it is not equivalent to using a size distribution. Also by fixing the radius for NAT, the sedimentation velocity is the same for all NAT particles, while for a size distribution the sedimentation velocity would be also a distribution. . .. So to my opinion, the inclusion of a size distribution for all PSC particles would give a more realistic approach and would not make the calculations much more time consuming.
Thanks for the question. The reason for adding the noise level of the satellite data to the results of the Mie and T-matrix calculations is that the satellite observations include significant uncertainty, i.e. a CALIPSO measurement of even a monodisperse PSC distribution would show a lot of scatter. To mimic these observational uncertainties we added the instrumental noise to our results.
Concerning the distribution of sedimentation velocities, we agree that there might be better approaches to describe the size distribution of PSC particles. However, the purpose of this paper is not to come up with a microphysically fully consistent PSC size distribution, but to evaluate and optimize the existing parameterization. Instead of fixing the NAT radius, other models fix the NAT number density (e.g. Wegner et al., 2013, Nakajima et al., 2016), which results in varying NAT radius and sedimentation velocities. However, the value for NAT number density is the model dependent and acts as tuning parameter. In reality, the actual value for NAT number density is far from being constant, because the active sites for NAT nucleation themselves show a wide distribution of efficacies (Hoyle et al., 2013). Therefore, we follow a different approach and choose a NAT radius to reasonably simulate the observed sedimentation/denitrification features.

I don't understand "but at the end of each chemical time step all condensed HNO3 and H2O evaporates back to the gas phase."

This means that the NAT and water ice particles are not themselves prognostic variables and are not explicitly transported by the model's advection scheme. This is a common approach in CCMs. At the end of the chemistry routine, the condensed HNO3 and H2O is returned to the gas phase and the transport occurs via the gas phase. At the next call of the chemistry scheme, NAT is freshly formed if the partial pressure of HNO3 exceeds supersaturation, and the particles are re-established within this equilibrium scheme. The same holds for water ice and the partial pressure of H2O. This procedure prevents numerical diffusion of within and between model grid cells of HNO3 and H2O, as PSC clouds are regionally limited and show strong gradients.

We rephased the sentence for clarification.

References:

Carslaw, K. S., Luo, B. P., and Peter, T.: An analytic expression for the composition of aqueous HNO3–H2SO4 stratospheric aerosols including gas-phase removal of HNO3, Geophys. Res.Lett., 22, 1877–1880, 1995.

Fahey, D. W., Gao, R. S., Carslaw, K. S., Kettleborough, J., Popp, P. J., Northway, M. J., Holecek, J. C., Ciciora, S. C., McLaugh-lin, R. J., Thompson, T. L., Winkler, R. H., Baumgardner, D. G., Gandrud, B., Wennberg, P. O., Dhaniyala, S., McKinney, K., Peter, T., Salawitch, R. J., Bui, T. P., Elkins, J. W., Webster, C. R., Atlas, E. L., Jost, H., Wilson, J. C., Herman, R. L., Kleinböhl, A., and von König, M.: The detection of large HNO3-containing particles in the winter arctic stratosphere, Science, 291, 1026–1031, https://doi.org/10.1126/science.1057265, 2001.

Hoyle, C. R., Engel, I., Luo, B. P., Pitts, M. C., Poole, L. R., Grooß, J.-U., and Peter, T.: Heterogeneous formation of polar stratospheric clouds- Part 1: Nucleation of nitric acid trihydrate (NAT), Atmos. Chem. Phys., 13, 9577–9595, https://doi.org/10.5194/acp-13-9577-2013, 2013.

Nakajima, H., Wohltmann, I., Wegner, T., Takeda, M., Pitts, M. C., Poole, L. R., Lehmann, R., Santee, M. L., and Rex, M.: Polar stratospheric cloud evolution and chlorine activation measured by CALIPSO and MLS, and modeled by ATLAS, Atmos. Chem. Phys., 16, 3311–3325, https://doi.org/10.5194/acp-16-3311-2016, 2016.

Pitts, M. C., Poole, L. R., Dörnbrack, A., and Thomason, L.W.: The 2009–2010 Arctic polar stratospheric cloud season: a CALIPSO perspective, Atmos. Chem. Phys., 11, 2161–2177, https://doi.org/10.5194/acp-11-2161-2011, 2011.

Wegner, T., D. E. Kinnison, R. R. Garcia, and S. Solomon (2013), Simulation of polar stratospheric clouds in the specified dynamics version of the whole atmosphere community climate model, J. Geophys. Res. Atmos., 118, 4991–5002, doi:10.1002/jgrd.50415.

Reply to the comment of Referee 2

We would like to thank the referee for taking the time to read our manuscript and for the helpful feedback. We have taken these comments into account and present our responses below, with reviewer comments in blue and author responses in black. The major changes to our manuscript, as suggested by the reviewer, are:

- Additional model simulations and analyses for the Antarctic winters 2006 and 2010, which represent years with above- and below-average PSC occurrence.
- Additional sensitivity simulations to investigate the impact of the model's cold bias on PSC formation: temperature for PSC formation increased by 3K.
- Extended discussion on further influencing factors for PSC formation like model resolution or temperature biases as well as of previous studies.

Steiner et al. present an evaluation of PSCs simulated with the CCM SOCOL by comparing these to the backscatter observations derived with CALIOP onboard CALIPSO. The comparison is performed for the Antarctic winter 2007 and simulation performance has been tested by using different microphysical properties to optimize the set-up for the PSC scheme.
This is a quite interesting study and could definitely be useful for the modelling community. However, I am a bit disappointed with the outcome of this study. At the end, with none of the used set-up a really good agreement with observations is found so that not really a recommendation for the modelling community can be given. On top of that the impact on the results for ozone (which was used as a motivator for this study) is not there at all. After major revisions the manuscript may be suitable for publication. Detailed comments for improvement are provided below.
In this study we performed the first in-depth evaluation of PSC occurrence and composition in the SOCOL model. We agree that the comparison with the satellite data shows that the agreement is not perfect, but we believe that the modifications in the microphysical parameters have indeed resulted in a significantly improved agreement with the CALIPSO observations. The fact that polar ozone showed little response to the modifications in the PSC scheme was also a surprise to us. From the simulations with enhanced temperatures for PSC formation we saw a later onset of the PSC-season and a reduced PSC area, both of which is in better agreement with CALIOP observations. Consequently, the onset of O3 depletion is also delayed by slightly less than one month, however still earlier than in the MLS observations. This shows that further improvements of other parts of the model are necessary to reduce the disagreement with between modeled and observed ozone.

General comments:

Why has the Antarctic winter 2007 been chosen? Is this winter representative for Antarctic winters? Why is only one winter analysed on not several? From the simulations and observations more years should be available.
We have chosen 2007 since is a typical Antarctic year, with a steady vortex and PSCs from May to September. Furthermore, CALIOP data coverage was high and there was no impact of volcanic eruptions. However, it is absolutely true that, based on available observational data and low computational costs, more winters can be analyzed. In response to the reviewer's criticism, we additionally analyzed the years 2006 and 2010 (with above-average and below-average PSC occurrences, respectively). The analysis of these two additional winters showed very similar results as of 2007 in all comparisons

(geographic PSC-distribution, areal coverage, histograms, MLS-comparisons). The main results are the same as for 2007 and the analysis of these two additional winters has not lead to different conclusions. For this reason, we still show the results for the year 2007 in the result-section. However, all plots for the years 2006 and 2010 are included in the appendix of the paper.

The SOCOL data is modified so that it mimics what CALIPSO is measuring. However, since SOCOL has the much coarser resolution wouldn't it then better to try modify the CALIPSO data so that it rather mimics the SOCOL coarse resolution and therefore what SOCOL is simulating?
This is an important point. In the analysis of the spatial distribution, where we show the polar stereographic plots, this averaging of the CALIPSO measurements over the SOCOL grid boxes is already applied. Within this revision, we also apply a similar method for the areal coverage calculations. By doing so, we intend to show by how much the area calculation from the SOCOL grid boxes contributes to a larger area compared to the method applied by Pitts et al. (2018), especially as we already mentioned in the text that this difference may most likely cause some of the overestimation. Our goal is to calculate the area from the measurements and from the simulations as similar as possible. Therefore, we average the measurements over the SOCOL grid boxes over 12 hours (the output frequency of our simulations). Since not all grid boxes are overpassed within 12 hours, we set the PSC area in the remaining grid boxes to the mean PSC area in the overpassed grid boxes along the same latitude. The areal coverage calculated with this approach is larger than calculated by the method applied in Pitts et al. (2018), which is what we expected. We show this additional Subplot in Fig. 5. However, the simulated PSC area is still larger, which is due to the cold bias of the model. The PSC area from a sensitivity run with increased PSC formation temperature is also included in Fig. 5 to show the effect of the temperature bias on PSC area.

The results should be put in the context of results derived from other studies for discussing and understanding the differences between simulation and observation (e.g. Khosrawi et al. 2018 for the Arctic and the papers by Orr et al. 2015 for the Antarctic). Also the efforts done by the WACCM community to improve the PSC scheme could be helpful for the discussion (Wegner et al. 2013; Brakebusch et al. 2013).
We agree that so far our manuscript was mainly focused on the presentation of our own results. We have now extended our discussion section substantially and discuss several of the mentioned papers. However, it should be mentioned that all these models and their PSC scheme are (slightly) different or the studies focused on different winters/hemispheres. So a one-by-one comparison with our study is not always possible.

The underestimation of denitrification seems to be a general problem in GCMs. This underestimation was also found in Khosrawi et al. 2017 and 2018 comparing EMAC with MLS and still remained even with a higher resolution. In general you blame to often the coarse resolution, but forgot to consider that also deficiencies in the model physic play a role as the representation of dynamics (e.g. descend) and the interplay of the chemistry.
As mentioned above we have extended our discussion section substantially. We now compare our studies with previous papers and discuss the potential impact of various model deficiencies.
We fully agree with the reviewer. The studies by Khosrawi et al. provide very important insights also for our analysis, especially since the EMAC model and the SOCOL model are based on the same general circulation model, namely MA-ECHAM5. EMAC was found to suffer from an underestimation of downward transport inside the polar vortex, and Khosrawi et al. (2017) suggested this as likely reason for the underestimated polar vortex O3. We now compare our studies with previous papers and discuss the potential impact of various model deficiencies. See also below.

Specific comments:

P1, L2: The process of denitrification (namely sedimentation of PSC particles and thus HNO3 removal from this atmospheric layer) should be quickly explained (as has been done in the introduction).
Done.

P1, L18: Which resolution has been used? Add here T42L39.
Yes, T42L39 has been used. Information has been added.

P2, L31: I think there are even newer references. There is at least the paper by Nakajima et al. (2016).
We added the reference Nakajima et al. (2016).

P2, L40: Is there really no newer version of the PSC scheme? Please check.
To our knowledge there is no newer version. The paper by Nakajima et al. (2016) explicitly states that their results confirm the possibility of an ice-free nucleation mechanism of NAT involving solid particles as suggested by Hoyle et al. Furthermore, Nakajima et al. do not take sedimentation into account. However, we will add the citation.

P4, L 99: With satellite observations from which satellite? MLS? Please add this information.
Yes, from MLS observations. Information will be added.

P4, L108: Why is the hydrolysis of N2O5 important? This should be explained.
In general, the heterogeneous hydrolysis of N2O5 is an important and efficient loss process for NOx as it forms HNO3. The respective reaction in the gas phase is comparatively slow. The heterogeneous reaction is important in the troposphere in aerosol particles and cloud droplets, but also in the stratosphere on binary aerosol and PSC particles.
The sentence in our manuscript explicitly refers to the N2O5 hydrolysis on **tropospheric aerosols**, and was mainly added for the sake of completeness. For the present study, it is not of importance. Therefore, we removed the sentence.

P4, L113: PSC types. . .. . -> this is a repetition. This has already mentioned in the previous paragraph.
Sentence will be deleted.

P4, L128: ". . ..but at the end of each chemical time step all condensed HNO3 and H2O evaporates back to the gas phase". What do you mean with that? This is not realistic at all.
This means that the NAT and water ice particles are not explicitly transported by the model's advection scheme. This is a common approach in CCMs. At the end of the chemistry routine, the condensed HNO3 and H2O is re-evaporated and the transport occurs via the gas-phase. At the next call of the chemistry scheme, NAT is freshly formed if the partial pressure of HNO3 exceeds supersaturation. The same holds for water ice and the partial pressure of H2O. This procedure goes back to times when tracer transport was computationally expensive, with the goal to keep the number of prognostic tracers small. Furthermore, it prevents numerical diffusion as PSC clouds are regionally limited and show strong gradients.
We will rephrase the sentence for clarification.

P5, L134: Using 39 vertical levels is really coarse and what is the motivation for doing this. Several studies show that much better results are derived with a higher resolution and computer resources nowadays allow doing such simulations. Especially since you only consider one winter you could have easily done the simulations with a much better resolution. Especially, the coarse vertical resolution is a drawback. Why have you not used 90 levels? Using 90 levels significantly improves the results in the stratosphere.

Whether L90 leads to improvements compared to L39 clearly depends on the quantity. We do not see large differences in the simulated Brewer-Dobson-Circulation (w*) between L39 and L90. Furthermore, for the present study we used SOCOL in specified dynamics mode, and in SD mode there are no large differences in stratospheric dynamics between L39 and L90. The cold bias in the polar lowermost stratosphere is very similar in both vertical resolutions. Therefore, we do not expect large differences in the simulated PSCs between L39 and L90. This is also supported by the study of Khosrawi et al. (2017), who applied the EMAC model in L90, in T42 and in a much higher horizontal resolution of T106. Both model versions showed very similar differences to observations. This shows that a higher resolution is not necessarily the remedy for all model deficiencies.

Khosrawi, F., Kirner, O., Sinnhuber, B.-M., Johansson, S., Höpfner, M., Santee, M. L., Froidevaux, L., Ungermann, J., Ruhnke, R., Woiwode,W., Oelhaf, H., and Braesicke, P.: Denitrification, dehydration and ozone loss during the 2015/2016 Arctic winter, Atmospheric Chemistry and Physics, 17, 12 893–12 910, https://doi.org/10.5194/acp-17-12893-2017, https://acp.copernicus.org/articles/17/12893/2017/, 2017.

P9, L225: Much is attributed to the coarse resolution. However, why has such a coarse resolution been used? Why has not one of the used set-up been used for a simulation with a higher resolution to check what impact this would have?

See above. Furthermore, a change to higher horizontal resolutions would require a complete re-tuning of the model, which is out of the question, also because we are currently working on a new model generation, which will apply T63 as default horizontal resolution. However, even with T63 we will not fully resolve mountain waves.

P9, 234: PSC formation depends strongly on temperature. How well is temperature simulated in SOCOL?

As the majority of chemistry-climate models, SOCOL experiences a cold temperature bias in the polar stratosphere. A comparison with ERA-Interim on four different pressure levels is shown in the Figure below. Mostly, the temperature difference is between 2 and 4 K. To address your question and investigate the impact of the cold bias on PSC formation in the model, we ran two further sensitivity analyses during this revision. In both simulations, temperature for PSC formation was increased by 3K, once for the reference simulation and once for the S_n(ice),n(NAT,max) simulation. A discussion of the former simulation in terms of areal coverage and of latter simulation regarding the MLS-comparison has been added to the manuscript. The simulation is denoted as S_T,n(ice),n(NAT,max). With the increased PSC formation temperature, PSCs occur later and their area clearly decreased, as expected. The area of this new simulation agrees very well with the observed PSC area (with a similar method as for the simulation; see above). Figure 5 has been extended with these new results. The simulations with increased PSC formation temperature further show a later onset of denitrification and ozone depletion, both of which also is expected with PSC occurring later. However, towards the end of winter, the difference in HNO3 and O3 between the simulations with and without increased PSC formation temperature vanish. Further, the new simulation show almost no more dehydration since ice rarely forms with the

formation temperature increased by 3K. The Figures 7-9 now include the new simulation. It is important to highlight, that we didn't increase the temperature of the model itself, but just for the PSC formation (i.e. the tropical tropopause temperature and the related dehydration remain unchanged).

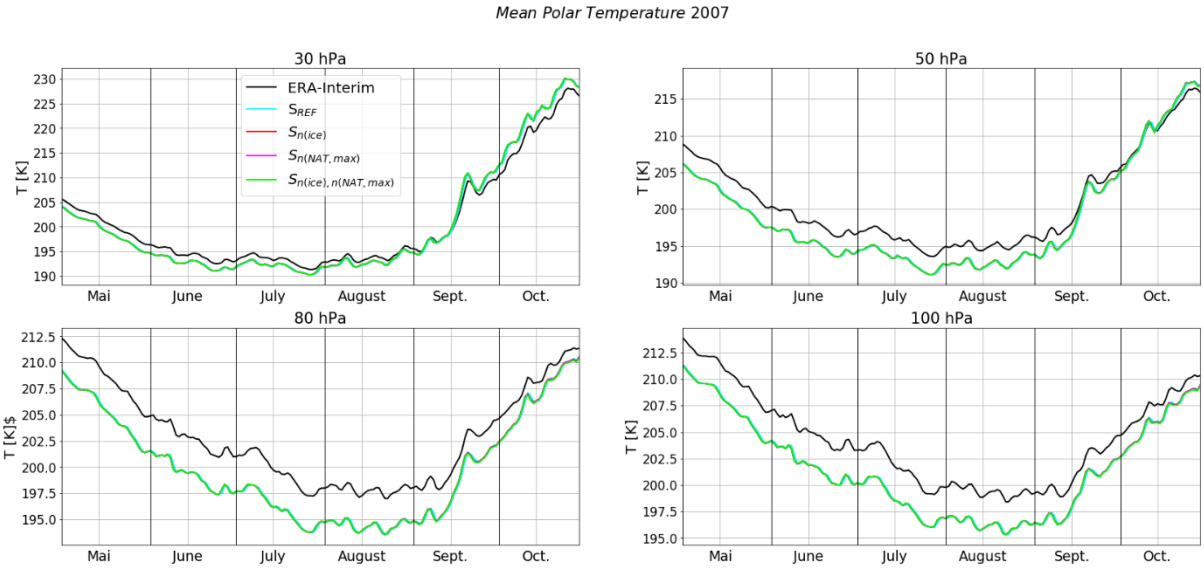

P12, Table 1: How are these values motivated? Have these been derived from the CALIPSO measurements or are these based on what is used in the literature (based on other observations or other experience with model simulations)?

The default setting for the microphysical parameters has been adopted from the previous model version SOCOL 2 (Schraner et al., 2008). The parameter settings for the sensitivity simulations have been defined based on the evaluation of the reference simulation with CALIPSO measurements and a stepwise modification of n_ice, n_nat_max and r_nat. We did many more simulations than presented in the paper, modified one parameter after the other and analyzed the impact of the respective parameter on the model result. It is clear that in reality PSCs are very heterogeneous in space and time, while a model like SOCOL has a coarse resolution, therefore, the "optimal" parameter setting is always a compromise and requires some testing and tuning. Furthermore, the "optimal" parameter setting will most likely depend on the model resolution or might change in future model versions with different dynamics, treatment of binary aerosol etc.

Schraner, et al., Technical Note: Chemistry-climate model SOCOL: version 2.0 with improved transport and chemistry/microphysics schemes, Atmos. Chem. Phys., 8, 5957–5974, https://doi.org/10.5194/acp-8-5957-2008, 2008.

P12, L274: Add references. At least there is a publication by Grooss et al. where a certain value for the ice number density has been used.

For example, Nakajima et al. (2016) also used 0.01 cm-3. Tritscher et al. (2019) used 10 cm-3 for homogeneous ice nucleation under mountain wave conditions. For heterogeneous ice nucleation they use a look-up-table (their Fig. 1) as done in Grooß et al. (2014) for NAT nucleation.

Grooß, J.-U., Engel, I., Borrmann, S., Frey, W., Günther, G., Hoyle,C. R., Kivi, R., Luo, B. P., Molleker, S., Peter, T., Pitts, M.C., Schlager, H., Stiller, G., Vömel, H., Walker, K. A., andMüller, R.: Nitric acid

trihydrate nucleation and denitrificationin the Arctic stratosphere, Atmos. Chem. Phys., 14, 1055–1073,https://doi.org/10.5194/acp-14-1055-2014, 2014.

Tritscher, I., Grooß, J.-U., Spang, R., Pitts, M. C., Poole, L. R., Müller, R., and Riese, M.: Lagrangian simulation of ice particles and resulting dehydration in the polar winter stratosphere, Atmos. Chem. Phys., 19, 543–563, https://doi.org/10.5194/acp-19-543-2019, 2019.

P13, L312: I do not really understand how this is done. How do you account for the heterogeneity of the MLS data by using area-weighted concentrations for SOCOL? How does that mimic the MLS measurements? Why not using the averaging kernels of MLS or just using the SOCOL output at the locations of the MLS measurements (thus along the satellite orbits)?

We average the MLS measurements over each SOCOL grid box, so that it makes the measurements comparable with SOCOL. To calculate the "polar mean" concentrations, the averaged MLS-values as well as the SOCOL concentrations are area-weighted to take into account the different areas of the grid boxes. We changed the sentence to: "To account for the spatial heterogeneity of the MLS measurements, we averaged the measurements over the SOCOL grid boxes from which area-weighted polar mean concentrations are calculated."

P16, L354 and 358: As stated in my general comments. The differences in agreement are partly caused by the coarse resolution. There are many other factors playing a role as well.

Agreed, and now considered in our discussion. See also next point.

P17, L369: But what is then the usefulness of this study? What would you recommend the modelers to do to improve their simulation results?

First, the main goal of the study was to evaluate the PSCs in the SOCOL model, which has never been done before to such an extent. As mentioned above, the fact that O3 did not react very much to the PSC modifications was also a surprise to us and suggests that other processes than heterogeneous chemistry play an important role for O3 in the polar stratosphere during winter/spring. As pointed out by Khosrawi et al. (2017) model deficiencies in downward transport inside the polar vortex are a promising candidate. As EMAC and SOCOL are both based on MA-ECHAM5 as underlying general circulation model, this might also hold for SOCOL. We mention this now in our discussion.
Second, all models are different. It is difficult to come up with a general suggestion for all modelers. Each has to be evaluated individually. We make this point when we put our results in context with other studies.

P17, L374: This is nothing new. This has also presented in other studies (e.g. Orr et al., Wegner et al., Brakebusch et al., Khosrawi et al .)

Agreed. We rephrased this sentence, pointing out that such simplified PSC schemes are widely used in the CCM community, however, with a wide range of assumptions concerning the microphysical parameters.

P1, L3: concentrations -> occurrences

Here we refer to polar ozone, not PSCs, so we think "concentrations" is correct.

P2, L41: PSCs are observed -> I that context I would rather write PSCs can be observed

Sentence has been changed.

P3, L84: The acronym MIPAS has not been introduced.
Acronym is now introduced.

P5, L140: 01 -> 1 (that should be changed in the text throughout the manuscript)
Corrected.

P6, L183-184: repetition of vertical resolution
Corrected.

P8, L213: 01 -> 1
Corrected.

P11, L250: 77.4-90◦ -> 77-90◦
We decided to stick to the notation of Pitts et al. (….), which is 77.8-90. Please note that the 77.4 has to read 77.8. This was a typo, which has been corrected. Thanks.

Figure A1 caption: 1st -> 1
Corrected.

Figure 2-9, A1: The resolution of the figures is not good enough. On my printed version the plot frames are missing in several occasions.
Thanks for this hint. We did not experience any problems with the figures, but we will clarify this issue with the GMD production office.

Figure 4: Swap the upper panels with the lower ones, so that the order is July, August. Why do you use SREF as figure title? Why not using “SOCOL” as figure title?
We used S_REF since the reference simulation (and not one of the sensitivity-runs) is shown. But it is absolutely correct, in the paper the Figure is shown before those sensitivity-simulations are introduced, so we changed the title. We further noticed that the plot were actually in the correct order (upper panel: July, lower panel: August), but the labels were swapped. This has been corrected. Thanks for pointing this out.

Figure 5: Here I would suggest to change the figure titles as follows: “CALIPSO”, “SOCOL with thresholds”, “SOCOL without thresholds”.
Done.

Figures 7 and 8: Observations and model simulations are difficult to distinguish. I would suggest to use a thicker line for the observations and maybe a different color.
We revised Figures 7-9 and changed the line thickness and colors.

Reply to Yunqian Zhu,

Dear Yunqian Zhu,

thank you very much for your helpful feedback. We appreciate your suggestions, which helped to improve our manuscript a lot. We present our point-by-point reply below, with your comments in blue and our responses in black.

Best regards,
Michael Steiner

Major comments:

I'm not convinced by your reasonable denitrification and ozone simulation right now (abstract Line 20). I think adding error bars (MLS accuracy) to the observation on your Figures 7, 8, and 9 may help to see whether the modeled HNO3, H2O, and O3 are reasonable. Right now, the onset of O3 depletion seems much earlier than the observation. This is important since the onset date of O3 depletion is one of the important indicators for ozone recovery (Solomon et al., 2016). Is your early O3 depletion caused by your early PSC formation that provides more SAD (Line 259)? I think your cold bias in the model may also contribute to both early PSC formation and early O3 depletion. If your model is not consistent with the O3 and other species after you add the error bars, you may want to emphasize your conclusion on "The change of NAT scheme has minimum impact on O3 depletion." And this conclusion is supported by previous studies like Tabazadeh et al.2000 which find the denitrification impact on Arctic ozone depletion but not much on the Antarctic one.

We added the MLS error bars to the Figures 7-9. While at the beginning of winter, O3 agrees well with observations, the difference between simulations and observations for HNO3 and H2O are large and also larger than the MLS uncertainty (upper panel). However, when looking at the relative evolution of the species (lower panel of the figures), the amplitude of denitrification and dehydration is in good agreement with observations, depending on the simulation. This is different for O3, where depletion in the model occurs too early and too strong, as you correctly stated. To test the hypothesis that the early onset of O3 depletion in the model is caused by early PSC formation, we ran sensitivity simulations with the temperature in the PSC routine constantly increased by 3K, which is roughly the temperature bias in the lower stratosphere. We indeed see a later onset of the PSC-season and a reduced PSC area, both of which is in better agreement with CALIOP-observations. As a consequence, the onset of O3 depletion is indeed delayed by slightly less than 1 month. However, this is still earlier than observed by MLS. Towards the end of the winter, the differences between the simulations vanish. The relatively small impact of the PSC scheme on the underestimation of O3 likely is a result of an underestimated downward transport inside the polar vortex. This is also discussed in the answers to the referee comment 2. We added this point to our discussion and included the fact, that modifications in the NAT scheme have minimal impact on O3, to our conclusions.

You explain your mismatching of PSCs to CALIPSO is due to the wave PSCs (e.g. Line 240, Line 245). I think the explanation is not enough. Why does the mountain wave cause higher R532? It is not just because of the wave-ice cloud, since wave ice clouds are a very small portion of PSCs. The large

R532 is likely to be enhanced-mix or ice clouds in CALIPSO observation. It is probably because you exclude NAT particles with higher number densities. These NAT particles are generated from ice or wave-ice cloud downwind the Antarctic Peninsula. Many observations saw or retrieved small NAT particles (~2 um) with large number densities, as well as the model simulations (see Zhu et al., 2017, and references therein, note that this is not the same paper you cited in this manuscript). Zhu, Y., Toon, O. B., Lambert, A., Kinnison, D. E., Bardeen, C., & Pitts, M. C. (2017). Development of a polar stratospheric cloud model within the Community Earth System Model: Assessment of 2010 Antarctic winter. Journal of Geophysical Research: Atmospheres, 122, 10,418– 10,438. https://doi.org/10.1002/2017JD027003 Line 295, I suggest you ran a test case with increased Sn(NAT, max) but decrease the NAT size.

Thank you very much for pointing this out. We agree with you that the upper limit for NAT number densities may contribute to the underestimation of the large R532 observations, and we added this point to the discussion of Fig. 4 and Fig. 6. However, we did not perform a further simulation with enhanced N(NAT,max) and smaller r(NAT). Even with such modified NAT parameters we would need some representation of the mountain waves in the model to reproduce these peaks. The observed clouds with enhanced-mix and ice downwind of the Peninsula form on ice which forms due to the mountain waves, and since mountain waves are almost not present in the simulation we would not see a peak downwind of the Peninsula. We would just shift the R532-values of all grid-boxes containing NAT particles. Furthermore, enhancing N(NAT,max) would put the reasonable agreement with the thin NAT-STS mixtures at stake.

Minor comments:

In the abstract, you mentioned meteoric dust as a possibility for PSC formation, but you haven't talked about it at all in the main content. Maybe put something in the discussion session.

We removed the meteoric dust from the abstract. Meteoric dust is not included in our model, and we think that a further discussion is beyond the scope of the paper.

Line 64, please cite Wegners et al., 2012 for PSC parameterization in WACCM

Reference added.

Line 65, I think Bardeen 2013 is not relevant.

We removed the citation.

Line 65 and 78-82, This is not the newest publication from Zhu et al. Please cite: Zhu, Y., Toon, O. B., Lambert, A., Kinnison, D. E., Bardeen, C., & Pitts, M. C. (2017). Development of a polar stratospheric cloud model within the Community Earth System Model: Assessment of 2010 Antarctic winter. Journal of Geophysical Research: Atmospheres, 122, 10,418– 10,438, https://doi.org/10.1002/2017JD027003. In this paper, we improved the model with ice to NAT nucleation. And the model is able to capture the small NAT particle features and compare pretty well with CALIPSO backscatter.

Thank you for the hint. We updated the reference and extended the description of the results for WACCM/CARMA.

Line 94, the equilibrium scheme is only for STS, but not for NAT and ice. Please rephrase here.

This is not quite correct. SOCOL does indeed assume equilibrium for STS, NAT and ice. Only if the NAT number density exceeds a certain threshold value, NAT deviates from equilibrium conditions.

Since the details of the PSC parameterizations are explained in Sect. 2.1, we decided to leave the respective sentence as is.

Line 119, could you provide a citation for “observational evidence”?
Observational evidence is for example given by the CALIPSO measurements, which show that NAT and STS occur at the same time (Pitts et al., 2011), which would not be possible without HNO3 supersaturation with respect to NAT. Further evidence is shown in the in situ study by Fahey et al. (2001): Fig. 5 D shows that the HNO3 supersaturation ratio with respect to NAT (Snat) was around 15 at the time the NAT particles where sampled (time = 0).

Line 140, instead of “average year”, you may say that 2007 is a typical Antarctic year with a steady vortex and observed PSCs from May to September. It is a year without the impact of volcanic eruptions. I think it would ask one question from another referee.
Thanks for the suggestion. We included this statement. Furthermore, we extended our analysis by the years 2006 and 2010, which represent years with above- and below-average PSC occurrence, but also without volcanic influence.

Line 194, please list citations for these refractive index numbers.
1.31 is simply the refractive index for water ice. For NAT, we added the following reference:

Middlebrook, A. M., Berland, B. S., George, S. M., Tolbert, M. A., and Toon, O. B.: Real refractive-indexes of infrared-characterized nitric-acid ice films – implications for optical measurements of polar stratospheric clouds, J. Geophys. Res., 99, 25655–25666, doi:10.1029/94JD02391, 1994.

Line 213, I think you mean “Figure 3d”
Corrected.

Figure 3a-c: these three figures have very different color bars. I cannot tell if you have a good comparison with CALIPSO or not. Instead of R532, you may use 1/R532 so you don’t have to compensate your color bar due to the wave-ice cloud. It’s up to you.
We adjusted the figure and use now 1/R532 as suggested.

Line 224 and 283, It is not due to "orography". It is due to the "lack of orographic gravity representation in the model".
Corrected.

Line 257, Is your CALIPSO figure identical with Pitts 2018? if so, Pitts 2018 says 77.8 rather than 77.4.
Thanks for spotting this mistake, we fixed it.

Line 265, “contributes to the larger PSC area and longer period”.
We adjusted the text accordingly.

Line 267-269, This sentence is not logical enough. Even you filtered it when you comparing to CALIPSO observation, you still count them into the SAD in your model, right? You may want to say “these STS clouds contribute to negligible SAD to the ozone chemistry in the model” if this statement is true.
You are absolutely right, the SAD of all PSC particles is counted in the model. With this sentence we wanted to state that the fact, that these large-scale STS clouds are almost entirely filtered out by the

thresholds, shows that these clouds must be teneous. We rephrased this sentence and tried to make the statement more clear:

“Those large-scale STS clouds are very tenuous since they are filtered out when applying the conservative PSC detection threshold. The contribution of those STS clouds to SAD is negligible."

Line 292, need a citation here for ice PSCs are less important for stratospheric ozone chemistry
We rephrased this statement and added a citation: “NAT PSCs play a twofold role in stratospheric ozone chemistry: Besides halogen activation on their surfaces, the sedimentation of NAT particles leads to denitrification, which hinders deactivation of reactive halogens and facilitates catalytic ozone loss (Peter, 1997).”

Line 320, “underestimates the HNO3 compared to MLS”
We adjusted the text accordingly.

References:

Fahey, D. W., Gao, R. S., Carslaw, K. S., Kettleborough, J., Popp, P. J., Northway, M. J., Holecek, J. C., Ciciora, S. C., McLaugh-lin, R. J., Thompson, T. L., Winkler, R. H., Baumgardner, D. G., Gandrud, B., Wennberg, P. O., Dhaniyala, S., McKinney, K., Peter, T., Salawitch, R. J., Bui, T. P., Elkins, J. W., Webster, C. R., Atlas, E. L., Jost, H., Wilson, J. C., Herman, R. L., Kleinböhl, A., and von König, M.: The detection of large HNO3-containing particles in the winter arctic stratosphere, Science, 291, 1026–1031, https://doi.org/10.1126/science.1057265, 2001.

Peter, T., Microphysics and heterogeneous chemistry of polar stratospheric clouds, Ann. Rev. Phys. Chem., 48, 785–822, 1997.

Pitts, M. C., Poole, L. R., Dörnbrack, A., and Thomason, L.W.: The 2009–2010 Arctic polar stratospheric cloud season: a CALIPSO perspective, Atmos. Chem. Phys., 11, 2161–2177, https://doi.org/10.5194/acp-11-2161-2011, 2011.

Reply to interactive comment by Astrid Kerkweg

Dear Dr. Kerkweg,

we fully understand the point that a permanent landing page allows for updating the contact information for the model source code, while this is not possible in a published paper.

Therefore, we have included the contact information for the SOCOLv3.1 model code to the zenodo repository (http://doi.org/10.5281/zenodo.4094663) and changed the code availability section accordingly. It now reads:

“Since the full SOCOLv3.1 code is based on ECHAM5, users must first sign the ECHAM5 license agreement before accessing the SOCOLv3.1 code (http://www.mpimet.mpg.de/en/science/models/license/, last access: 2020). Then the SOCOLv3.1 code is freely available. The contact information for the full SOCOLv3.1 code as well as the source code of the PSC module and the Mie and T-matrix scattering code are available at http://doi.org/10.5281/zenodo.4094663. …”

We hope this fulfills the requirements.

Please note that in addition we uploaded two zip-archives including coefficients for the T-matrix calculations that were missing in the initial repository. Therefore, the doi has changed.

Best regards,
Michael Steiner

Evaluation of polar stratospheric clouds in the global chemistry-climate model SOCOLv3.1 by comparison with CALIPSO spaceborne lidar measurements

Michael Steiner[1,*], Beiping Luo[1], Thomas Peter[1], Michael C. Pitts[2], and Andrea Stenke[1]

[1]Institute for Atmospheric and Climate Science, ETH Zurich, Switzerland
[*]now at Laboratory for Air Pollution / Environmental Technology, EMPA, Switzerland
[2]NASA Langley Research Center, Hampton, Virginia 23681, USA

Correspondence: Michael Steiner (michael.steiner@empa.ch)

Abstract. Polar Stratospheric Clouds (PSCs) contribute to catalytic ozone destruction by providing surfaces for the conversion of inert chlorine species into active forms and by denitrification~~of the stratosphere~~. The latter describes the removal of HNO_3 from the stratosphere by sedimenting PSC particles, which hinders chlorine deactivation by the formation of reservoir species. Therefore, an accurate representation of PSCs in chemistry-climate models (CCMs) is of great importance to correctly simulate polar ozone concentrations. Here, we evaluate PSCs as simulated by the CCM SOCOLv3.1 for the Antarctic ~~winter~~ winters 2006, 2007 and 2010 by comparison with backscatter measurements by CALIOP onboard the CALIPSO satellite. The year 2007 represents a typical Antarctic winter, while 2006 and 2010 are characterised by above- and below-average PSC occurrence. The model considers supercooled ternary solution (STS) droplets, nitric acid trihydrate (NAT) particles, water ice particles, and mixtures thereof. PSCs are ~~parametrized~~ parameterized in terms of temperature and partial pressures of HNO_3 and H_2O, assuming equilibrium between gas and particulate phase. ~~We use the CALIOP measurements to optimize three~~ The PSC scheme involves a set of prescribed microphysical parameters~~of the PSC scheme~~, namely ice number density, NAT particle radius and maximum NAT number density. In this study, we test and optimize the parameter settings by several sensitivity simulations. The choice of the ~~prescribed value of~~ value for the ice number density affects simulated optical properties and dehydration, while modifying the ~~maximum NAT number density or the NAT particle radius~~ NAT parameters impacts stratospheric composition ~~by enhancing the~~ via HNO_3-uptake and denitrification. Depending on the NAT-parameters, reasonable denitrification can be modeled. However, its impact on ozone loss is minor. Best agreement with the CALIOP optical properties and observed denitrification was for this case study found with the ice number density increased from the hitherto used value of 0.01 to 0.05 cm^{-3} and the maximum NAT number density from 5×10^{-4} to 1×10^{-3} cm^{-3}. The NAT radius was kept at the original value of 5 μm. The new parametrization reflects the higher importance attributed to heterogeneous nucleation of ice and NAT particles ~~, e.g. on meteoric dust,~~ following recent new data evaluations of the state-of-the-art CALIOP measurements. A cold temperature bias in the polar lower stratosphere results in an overestimated PSC areal coverage in SOCOLv3.1 by up to ~~100%.~~ 40%. Offsetting this cold bias by +3 K delays the onset of ozone depletion by about two weeks, which improves the agreement with observations. Furthermore, the occurrence of mountain-wave induced ice, as observed mainly over the Antarctic Peninsula, is continuously underestimated in the model due to the coarse model resolution (T42L39) and

the fixed ice number density. ~~However, overall we find a~~ Nevertheless, we find an overall good temporal and spatial agreement between modeled and observed PSC occurrence and composition~~, as well as reasonable modeled denitrification and ozone loss. Based on constraining three important parameters by means of the CALIOP measurements, this work demonstrates that also a simplified PSC scheme, which describes STS, NAT, ice and mixtures thereof with equilibrium assumptions and avoids~~ . This work confirms previous studies that also simplified PSC schemes, which avoid nucleation and growth calculations in sophisticated, but time-consuming microphysical process models, may achieve good approximations of fundamental properties of PSCs needed in CCMs.

1 Introduction

Although the occurrence of clouds in the wintertime polar stratosphere has been observed for a long time, their importance for stratospheric ozone depletion was only recognized after the discovery of the Antarctic ozone hole in the mid 1980s (Farman et al., 1985). Stratospheric clouds composed of supercooled ternary solutions (STS, H_2SO_4-HNO_3-H_2O mixtures), crystalline nitric acid trihydrate (NAT) and water ice provide surfaces, on which inert reservoir species like HCl and $ClONO_2$ are transformed into active forms (Solomon et al., 1986). The activated species then are responsible for springtime ozone depletion induced by catalytic cycles (Molina and Molina, 1987). While STS droplets are responsible for most of the chlorine activation ~~(Portmann et al., 1996; Kirner et al., 2015, and references therein)~~ (Portmann et al., 1996; Kirner et al., 2015; Nakajima et al., 2016, and references therein), solid particles can in addition strongly affect the chemical composition of the stratosphere. Especially NAT particles can, under certain conditions, grow to large particles with diameters of up to 20 μm, so-called NAT-rocks (Fahey et al., 2001). Their number density is small (Biele et al., 2001), but due to their size they reach high settling velocities and by sedimentation remove reactive nitrogen from the stratosphere. This so-called denitrification contributes to ozone depletion by hindering the formation of inactive reservoir species (Salawitch et al., 1993).

While the formation of water ice requires extremely cold conditions in the dry stratosphere, HNO_3-containing particles already occur at higher temperatures (Hanson and Mauersberger, 1988), and hence much more frequently. In contrast to solid particles, there is no nucleation barrier for liquid STS droplets, which form upon uptake of HNO_3 and H_2O from the gas-phase by binary H_2SO_4-H_2O solution droplets (Carslaw et al., 1995). Depending on the presence or absence of heterogeneous nuclei, different pathways of PSC formation exist (e.g. Fig. 2 in Hoyle et al., 2013).

PSCs ~~are~~ can be observed by ground-based lidar instruments (e.g. Biele et al., 2001; Simpson et al., 2005), in airborne campaigns (e.g. Fahey et al., 2001) or by space-borne satellites ~~(e.g. Michelson Interferometer for Passive Atmospheric Soundings; Fischer and Oelhaf, 1996; Fischer et al., 2008)~~ (e.g. Michelson Interferometer for Passive Atmospheric Soundings (MIPAS); Fischer and Oelhaf, 1996; Fischer et al., 2008). Since 2006 the Cloud-Aerosol Lidar with Orthogonal Polarization (CALIOP) on CALIPSO (Cloud-Aerosol Lidar and Infrared Pathfinder Satellite Observations) measures PSCs with high vertical resolution (Winker and Pelon, 2003; Winker et al., 2007, 2009; Pitts et al., 2018). CALIOP measures backscatter intensities at 532 nm and 1064 nm wavelength, and additionally

separates the 532 nm backscatter signal into parallel and perpendicular polarized components. The depolarization ratio is a measure of the particle shape and allows to distinguish between liquid (spherical) and solid (aspherical) particles. This makes CALIOP a very suitable tool for observing and classifying PSCs.

Due to their critical role in stratospheric chemistry, the representation of PSCs is indispensable for atmospheric chemistry models. However, the complexity of PSC schemes varies considerably between models. Some models primarily aim at mimicking the effects of PSCs on chemical composition and vertical re-distribution of HNO_3 and H_2O rather than at exactly reproducing PSC compositions. The detailed PSC formation along different pathways, depending on the presence or absence of heterogeneous nuclei, is usually not taken into account in those models. This is no problem under many circumstances, e.g. when chlorine activation is close to saturation in the middle of an Antarctic winter, but an accurate knowledge of the heterogeneous reaction and denitrification rates is essential for a quantitative description of polar ozone chemistry under transitional conditions, as they occur at winter onset or in late winter and early spring, or at the far edge of the vortex. Therefore, some models include PSCs in a more sophisticated manner and aim at correctly simulating nucleation, growth and sedimentation of the different PSC types as well as the detailed redistribution of HNO_3 and H_2O.

Simple parametrizations form NAT or ice instantaneously either at the saturation temperature, or at a certain supersaturation. Below the onset temperature of NAT or ice, excess matter of HNO_3 or H_2O is directly transferred into the particulate phase, assuming equilibrium. The particle size then depends on assumptions made about the number density distribution or vice versa. Examples for global chemistry models using such PSC parametrizations are SOCOLv3.1 (Stenke et al., 2013), LMDZrepro (Jourdain et al., 2008) or CCSRNIES (Akiyoshi et al., 2009). More complex PSC schemes allow deviations from thermodynamic equilibrium and explicitly simulate nucleation, growth and evaporation of particles, as in CLaMS (Tritscher et al., 2019) or WACCM/CARMA ~~(Garcia et al., 2007; Bardeen et al., 2013; Zhu et al., 2017b)~~ (Garcia et al., 2007; Wegner et al., 2012; Zhu et al., 2017a). As particle sedimentation is important for the chemical composition of the stratosphere, it is included in all PSC schemes. The settling velocity is mainly dependent on particle size, which is either described by a modal size distribution (e.g. SOCOL, LMDZrepro), size bins (e.g. ~~SWACCM~~WACCM/CARMA, EMAC (Khosrawi et al., 2018), BIRA (Daerden et al., 2007)) or as single representative particles in models with Lagrangian sedimentation schemes (e.g. SCLaMS, ATLAS (Wohltmann et al., 2010), SLIMCAT/TOMCAT (Feng et al., 2011)). A detailed overview over the representation of PSCs in global models and its evaluation can be found in ~~Grooß et al. (2020, in prep.)~~ Grooß et al. (2020, under review).

Different approaches have been used to investigate the performance of PSC schemes, ranging from the evaluation of bulk properties like PSC areal coverage or air volume covered by PSCs up to detailed assessments of PSC properties along single satellite orbits. In addition, the ~~impacts~~ impact of PSCs on the chemical composition or chlorine activation can be evaluated by comparison with observations of certain chemical species. Tritscher et al. (2019) recently presented a detailed evaluation of PSCs in CLaMS, including optical properties, geographical PSC volume, along-orbit comparisons and influence on gas-phase HNO_3 and H_2O. Simulations for the Arctic winter 2009/2010 and the Antarctic winter 2011 show good agreement with observations. However, the simulated HNO_3-uptake in early winter was stronger than observed and the permanent redistribution of HNO_3 was underestimated. A new PSC model in WACCM/CARMA, taking into account detailed microphysical processes,

was presented by Zhu et al. (2017b) ~~. They extensively compared the PSCs in the~~ and Zhu et al. (2017a). For the Antarctic winter 2010~~with CALIOP-observations and examined modeled gas-phase and distributions. They found the derived~~ , they found the optical properties of ~~PSCs and the denitrification to be well~~ the simulated PSCs to compare well with CALIOP-observations. Also observed denitrification was well reproduced by the model. ~~However,~~ After implementing ice nucleation on NAT and vice versa, the model is now able to capture PSCs with small NAT particles and large number densities ~~were underestimated, which might be caused by a missing NAT formation pathway on ice particles (Zhu et al., 2017b)~~as well. Other studies focused mainly on the impact of PSCs by comparing HNO_3 and H_2O with space-borne observations from MLS (Microwave Limb Sounder; Waters et al., 2006; Schoeberl, 2007), MIPAS or with airborne measurements. The study by Khosrawi et al. (2018), evaluating EMAC for the Arctic winters 2009/2010 and 2010/2011, found good agreement for the temporal evolution of gas-phase HNO_3 in the polar stratosphere, but simulated PSC volumes were smaller than observed by MIPAS. Recently, Snels et al. (2019) presented a statistical comparison including several models from CCMVal-2 and CCMI project with observations. They used a set of diagnostics, based on spatial distribution of ice and NAT surface area densities and temperature, to compare simulated PSCs among the different CCMs. They concluded that the geographical distribution of PSCs in the polar vortex, as observed by CALIOP, is not well reproduced by the models. The models showed ~~a~~ limited ability to reproduce the longitudinal variations in PSC occurrences and mostly overestimate NAT and ice occurrence, most probably due to a cold temperature bias. WACCM-CCMI (Garcia et al., 2017), where the cold bias was reduced by introducing additional mechanical forcing of the circulation via parametrized gravity waves, compared best with observations.

In this study, we compare a simple equilibrium scheme of STS, NAT, ice and mixtures thereof with state-of-the-art PSC satellite data, aiming to optimize the scheme for economic and efficient use in a chemistry-climate model (CCM). To this end, we evaluate the representation of PSCs in the CCM SOCOLv3.1 for the Antarctic ~~winter 2007.~~ winters 2006, 2007 and 2010. We convert the simulated PSCs into an optical signal to mimick a satellite measurement and compare the results with CALIPSO observations. We further evaluate the impacts of the simulated PSCs on the chemical composition of the stratosphere by comparison with ~~satellite~~ MLS-satellite observations of HNO_3, H_2O and O_3. A more detailed description of our methodology and the datasets utilized is given in Sect. 2. In Sect. 3 we present the results of the comparison, and Sect. 4 provides conclusions.

2 Model description and observational data

2.1 The SOCOLv3.1 chemistry-climate model

The state-of-the-art chemistry-climate model SOCOLv3.1 (Stenke et al., 2013; Revell et al., 2015) is based on the middle-atmosphere general circulation model (GCM) MA-ECHAM5 (European Centre/HAMburg climate model; Roeckner et al., 2006), coupled to the chemistry module MEZON (Model for Evaluation of oZONe trends; Egorova et al., 2003). MEZON contains 57 chemical species, 56 photolysis reactions, 184 gas-phase reactions and 16 heterogeneous reactions in and on aqueous sulfuric acid aerosols (supercooled binary solutions, SBS) as well as three types of PSCs, namely STS droplets, NAT and water ice. ~~Heterogeneous hydrolysis of on tropospheric aerosols is as well taken into account.~~ The chemistry module MEZON

covers stratospheric ozone chemistry in detail as well as the tropospheric background chemistry, including the oxidation of isoprene (Pöschl et al., 2000). The coupling between the GCM and the chemistry module takes place through simulated winds and temperatures, as well as through the radiative forcing caused by ozone, methane, nitrous oxide, water vapor and CFCs. The dynamical time step is 15 min, whereas the radiation and chemistry schemes are called every 2 h.

~~The parametrization of PSCs in MEZON includes the three PSC types water ice, NAT and STS . STS~~ In SOCOLv3.1, STS droplets form upon the uptake of gas-phase HNO_3 and H_2O by aqueous sulfuric acid aerosols~~(supercooled binary solutions, SBS),~~, following the expression by Carslaw et al. (1995). ~~In SOCOLv3.1, the~~ The binary aerosols are prescribed ~~as a time series of observed monthly mean sulfate aerosol surface area density~~from a monthly mean observational data record, mainly based on SAGE (Stratospheric Aerosol and Gas Experiment) observations~~(Stenke et al., 2013).~~ . This data set was prepared for CMIP6 (Eyring et al., 2016), and provides surface area density (SAD), volume density, mean radius and H_2SO_4 mass of the binary aerosol. The uptake of HNO_3 and H_2O leads to a change in aerosol mass, from which a growth factor for the SBS particles and, therefore, the STS particle size is calculated. The stratospheric aerosol data set and its description can be found at ftp://iacftp.ethz.ch/pub_read/luo/CMIP6/.

NAT is formed if the HNO_3 partial pressure exceeds its saturation pressure (Hanson and Mauersberger, 1988). For NAT particles, ~~a mean radius of 5 is assumed, and~~ we fix the mean radius and limit the maximum number density~~is set to $5{\cdot}10^{-4}$. This limitation~~ . The latter accounts for the ~~observational evidence that NAT clouds are often strongly supersaturated~~ fact that NAT and STS clouds are mostly observed simultaneously (e.g., Pitts et al., 2011), and prevents condensation of all available gas-phase HNO_3 onto NAT particles ~~. The assumptions of~~ at the expense of STS formation. In the reference set-up, we assumed a mean radius (r_{NAT}) of 5 µm and a maximum number density ($n_{NAT,max}$~~=~~) of $5{\cdot}10^{-4}$ cm^{-3} ~~and r_{NAT}=5~~ (Table 1). These settings allow for ∼10% of the HNO_3 at beginning of winter to be taken up into NAT particles (0.77 ppbv at 50 hPa and 195 K, assuming 5 ppmv H_2O).

For water ice, ~~a~~ we prescribe the particle number density (n_{ice}). The reference setting of 0.01 cm^{-3} ~~is prescribed. This represents the background ice number density~~ represents background conditions, but not ice ~~formed in~~ clouds formed due to mountain waves, where very high nucleation rates result in much higher ice number densities of ∼ 5-10 cm^{-3} (Hu et al., 2002) and particle sizes of <3 µm (Höpfner et al., 2006). ~~For water ice particles as well as~~ As for STS droplets the PSC routine assumes the water ice particles to be in thermodynamic equilibrium with the gas-phase.

The different treatment of NAT and water ice in the SOCOL model is motivated by the respective timescales to reach equilibrium between particulate and gas-phase. For water ice, this timescale is very short. Once ice has formed, further cooling leads rather to particle growth than to additional nucleation of fresh particles. In case of NAT, however, the equilibrium between particulate and gas-phase is hardly reached, as shown by observations (e.g., Fahey et al., 2001), and additional particles can nucleate upon further cooling.

Sedimentation of solid PSC particles is included in the model. The fall velocities of NAT and ice particles are based on Stokes theory (described in Pruppacher and Klett, 1997). ~~Advection of PSC particles is not explicitly calculated in SOCOL, but at~~ NAT and ice PSCs are not explicitly transported in SOCOL. At the end of ~~each chemical time step~~ the chemistry routine all condensed HNO_3 and H_2O evaporates back to the gas phase. This means that at each call of the chemistry routine NAT

and ice PSCs (re-)form instantaneously depending on the prevailing partial pressures of HNO_3 and H_2O, respectively. This approach avoids undesired numerical diffusion due to the spatial heterogeneity in PSC occurrence. To prevent spurious PSC formation caused by potential model temperature, HNO_3 and/or H_2O biases in regions where PSCs are usually not observed, and to avoid overlap with the regular cloud scheme of the GCM, the occurrence of PSCs is spatially restricted. Water ice particles are allowed to occur between 130 hPa and 11 hPa and polewards of 50°N/S. NAT particles are allowed between the tropopause and 11 hPa. STS and NAT particles may form at all latitudes.

For the present study SOCOLv3.1 was run with T42 horizontal resolution (about 2.8°x 2.8°in latitude and longitude) and 39 vertical levels between the surface and the model top centered at 0.01 hPa (∼80 km). In order to allow for a direct comparison with observations, the model was run in specified dynamics mode, i.e. the prognostic variables temperature, vorticity, divergence and the logarithm of the surface pressure are relaxed towards ERA-Interim reanalysis data (Dee et al., 2011). We applied a uniform nudging strength throughout the whole model domain, with a relaxation timescale of 24 h for temperature and logarithm of the surface pressure, 48 h for divergence and 6 h for vorticity. The boundary conditions follow the specifications of the reference simulation REF-C1 of phase 1 of the Chemistry Climate Model Initiative (CCMI-1; Morgenstern et al., 2017). All simulations for this study were run ~~between 01 May 2007 and~~ for the time period from 1 May to 31 October ~~2007~~ with a 12-hourly output time step. We chose the years 2006, 2007 and 2010 for our evaluation~~, which represents an average winter in terms of~~ . While 2007 represents a typical Antarctic year with a steady vortex and PSCs observed from May to September, 2006 and 2010 are years with above- and below-average PSC occurrence, ~~while data coverage for CALIPSO was rather high.~~ respectively. All years are without volcanic influence.

2.2 CALIPSO PSC observations

The simulated PSCs in SOCOL are compared to measurements from the CALIOP instrument onboard CALIPSO, an Earth observation satellite in the A-train constellation in operation since 2006 (Winker and Pelon, 2003; Winker et al., 2007, 2009). The A-train of satellites orbits the Earth 14-15 times per day, covering the latitudes between 82°S and 82°N on each orbit. CALIOP is a dual-wavelength lidar with three receiver channels, one measuring the 1064 nm backscatter intensity, the two others measuring the parallel and perpendicular polarized components ($\beta_{\parallel}$ and $\beta_{\perp}$) of the 532 nm backscattered signal. The frequency of the lidar pulse is 20.25 Hz, corresponding to one measurement every 333 m along the flight track. From the measured backscatter coefficients (e.g. β_{532}) the total (sum of particulate and molecular) to molecular backscatter ratio

$$R_{532} = \frac{\beta_{532}}{\beta_{\mathrm{m}}} = \frac{\beta_{\mathrm{part},532} + \beta_{\mathrm{m}}}{\beta_{\mathrm{m}}} \tag{1}$$

can be calculated, with β_{m} being the molecular backscatter coefficient. β_{m} is calculated as described in Hostetler et al. (2006), using molecular number density profiles provided by the MERRA-2 (Modern-Era Retrospective analysis for Research and Applications, version 2) reanalysis products (Gelaro et al., 2017). With the separation of the 532 nm backscatter signal into parallel and perpendicular polarized components, the depolarization ratio ~~(~~$\delta_{\mathrm{aerosol}}$ ~~, i.e. the (~~perpendicular to parallel component) of the 532 nm signal can be derived, which is an indicator of the particle shape and hence phase (liquid/solid).

In this study, we use the Lidar Level 2 Polar Stratospheric Cloud Mask Product (available via Michael C. Pitts), which was derived with version 2 (v2) of the PSC detection algorithm (Pitts et al., 2018) from the CALIOP v4.10 Lidar Level 1B data products. This CALIOP PSC dataset contains profiles of PSCs with classification and optical properties, also providing temperature, pressure and tropopause height derived from MERRA-2 reanalyses. The spatial resolution of PSC data is 5 km in the horizontal by 180 m in the vertical. Only night-time measurements are considered. ~~For this study, CALIPSO data from 01 May 2007 to 31 October 2007 are used.~~

Version 2 of the detection algorithm (Pitts et al., 2018) detects PSCs as statistical outliers in either $\beta_\perp$ or R_{532}, relative to the background stratospheric aerosols population. The optical properties of stratospheric background aerosol are derived from CALIOP measurements above 200 K. Both thresholds are defined as median plus one median absolute deviation. ~~They are calculated daily~~ The values are calculated on a daily basis and vary with potential temperature. Furthermore, additional horizontal averaging (over 15, 45 and 135 km) has been implemented into the PSC detection algorithm to enable the detection of more tenuous clouds than at 5 km resolution only.

The PSC classification in Pitts et al. (2018) distinguishes STS, STS-NAT mixtures, enhanced NAT mixtures, ice and wave ice. The categories are visualized in Fig. 1. The dotted lines denote dynamical boundaries, while the solid lines show boundaries at fixed $\beta_\perp$ or R_{532} values. The lines at the lower left corner approximate the $\beta_\perp$-threshold ($\beta_{\perp,\text{thresh}}$) and R_{532}-threshold ($R_{532,\text{thresh}}$), respectively. All PSCs above $\beta_{\perp,\text{thresh}}$ are assumed to contain non-spherical particles. The boundary between the two NAT mixture categories and ice is calculated "dynamically", i.e. based on cloud-free MLS measurements of HNO_3 and H_2O. PSCs are detected as wave ice when they contain non-spherical particles and if R_{532}>50. A detailed description of the classification scheme is given in Pitts et al. (2018). PSC observations of July 2007 (Fig. 1) show the most distinct relative maxima for STS. Two further relative maxima appear with higher δ_{aerosol} values, indicating solid particles. The relative maximum extending towards the upper left corner of the histogram corresponds to STS-NAT mixtures with low NAT number densities (n_{NAT}), while the second relative maximum extending towards the upper right corresponds to mixtures of NAT with high number densities and ice as well as to wave ice PSCs.

2.3 MLS observations

In this study, modeled HNO_3, H_2O and O_3 mixing ratios are compared to satellite measurements of the ~~instrument~~ Microwave Limb Sounder (MLS) onboard the Aura satellite (Waters et al., 2006). MLS measures atmospheric profiles by scanning from the ground to 90 km height in flight direction, passively measuring microwave thermal emissions. All three quantities are derived by version 4.2 from the Aura MLS Level 2 data (Livesey et al., 2018). The HNO_3 dataset has a vertical resolution of approximately 3-4 km~~vertical resolution~~, while the H_2O and O_3 datasets have a vertical resolution of 2.5 to 3 km. The accuracy of the MLS measurements is 1-2 ppbv for HNO_3 (Santee et al., 2007), 4%-7% for H_2O (Read et al., 2007; Lambert et al., 2007) and 8% for stratospheric O_3 (Jiang et al., 2007). Detailed informations and a precise description of the dataset can be found in Livesey et al. (2018).

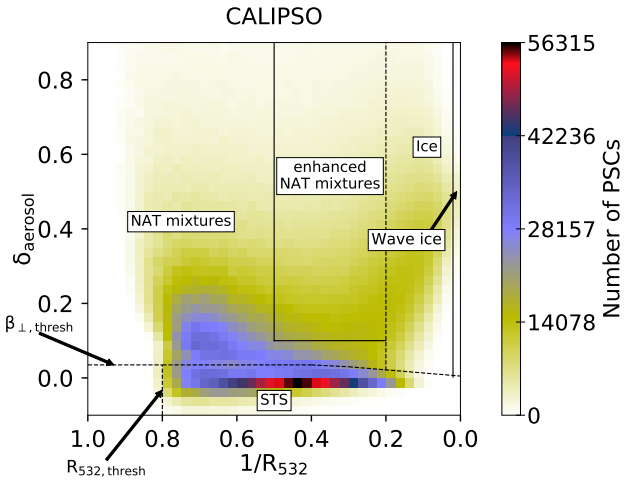

Figure 1. Composite 2D-histogram of CALIPSO PSC measurements of July 2007 in a $1/R_{532}$-δ_{aerosol} coordinate system with 40x40 bins. The colors indicate the number of PSC measurements in one bin. Dotted lines denote dynamical classification boundaries or thresholds and solid lines denote fixed classification boundaries.

2.4 Model-measurement comparison

While CALIOP measures backscatter signals and depolarization ratios, the SOCOL model provides surface area densities ~~(SAD)~~ for STS, NAT and water ice as function of pressure, latitude and longitude. From the ~~simulated SADs and the assumed~~ outputted SADs of the three PSC types and the prescribed microphysical parameters, i.e. r_{NAT} and n_{ice}, as well as the growth factor for liquid aerosols we calculate the number density and/or radius for each particle type. ~~This information is~~ These quantities are used in Mie and T-matrix scattering codes (Mishchenko et al., 1996) to compute optical parameters of the simulated PSCs, i.e. R_{532}, δ_{aerosol} and $\beta_{\perp}$, for comparison with CALIOP observations. For NAT and ice particles, circular symmetric spheroids with an aspect ratio of 0.9 are assumed. Refractive indices of 1.31 for water ice and 1.48 for NAT (Middlebrook et al., 1994) were chosen. STS are liquid particles and therefore assumed to be spherical, which corresponds to a depolarization ratio $\delta_{\text{aerosol}} = 0$.

The CALIOP PSC data product includes ~~both detection threshold values~~detection thresholds, $R_{532,\text{thresh}}$ and $\beta_{\perp,\text{thresh}}$, for each measurement. ~~To achieve a better comparability between model and observations, these daily threshold values are also applied on~~ As the geographical PSC extent strongly depends on these detection limits, they have to be applied to the calculated optical properties of the ~~PSCs simulated by SOCOL~~simulated PSCs as well to ensure a fair comparison between model and satellite data. For this purpose, we calculated for each pressure level the daily mean thresholds ~~from all observationsfor each pressure level. This procedure is essential for a fair comparison between model and satellite data, as the geographical PSC extent strongly depends on these detection limits.~~ over all observations.

The satellite measurements are subject to uncertainties. Even for a perfectly monodisperse PSC distbution a CALIPSO measurement would show some scatter. To ensure best possible comparability between model and measurements, observational

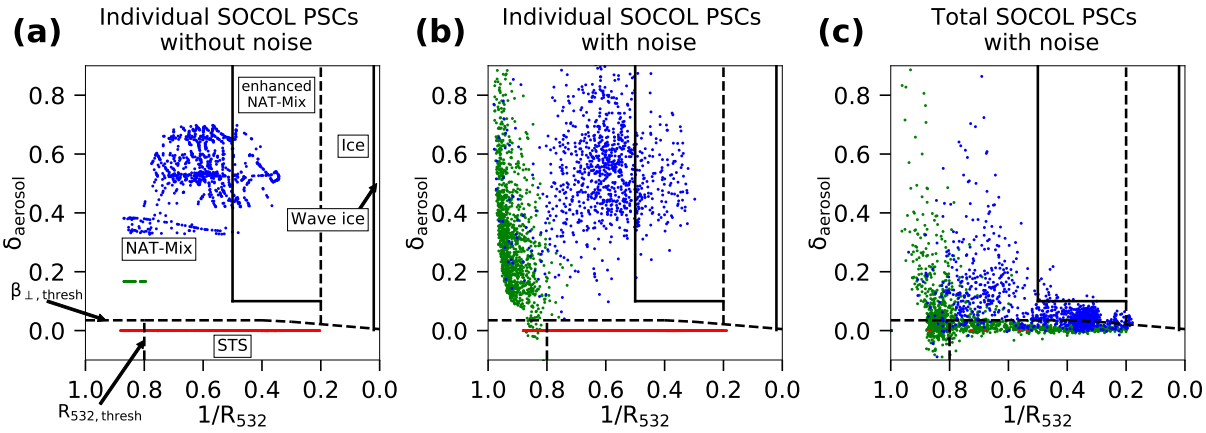

Figure 2. Scatter plot of simulated PSCs ~~in~~ from the SOCOL simulation S_{REF} on ~~01~~ 1 July 2007 in a $1/R_{532}$-δ_{aerosol} coordinate system. (a): STS (red), NAT (green) and ice (blue) as individual components. (b): As in (a), but after applying observational uncertainties. (c): The modeled PSCs as mixture of all components present per grid box (red: pure STS, green: STS-NAT mixtures, blue: mixtures with ice) with uncertainty.

uncertainties have to be applied to the calculated optical properties of the modeled PSCs. We followed the approach by Engel et al. (2013). The uncertainty scales inversely to the square root of the horizontal averaging distance along a flight path, which we set to 135 km. This value corresponds to the best case for detection, which maximizes the comparability with the model (which obviously does not have a detection threshold). An example for the added measurement noise is shown in Fig. 2. When looking at the ~~individual PSC types~~ three PSC types individually (Fig. 2a), STS ~~and NAT,~~ (due to their ~~spherical shape and fixed radius,~~ assumed spherical shape) and NAT (due to the fixed radius) appear at constant δ_{aerosol}-values of 0 and 0.167, respectively. The variable radius of ice particles results in a variable δ_{aerosol}-value. Applying the uncertainties to the parallel and the perpendicular backscatter coefficients primarily causes a large spread in depolarization ratio (Fig. 2b). When considering all PSC particles to be mixed within a grid box (Fig. 2c), ~~their points are located~~ they appear mainly at the lower and left side of the composite histogram.

3 Results and discussion

Since our results and conclusions do not substantially differ for the three analyzed winters, we focus here on the year 2007, a typical Antarctic winter. Figures for the winters 2006 and 2010 are shown in the Appendix (Fig. A3-A14). We start with the analysis of our reference simulation (Table 1). The sensitivity simulations are discussed in Sect. 3.4.

3.1 Comparison along an orbit

As a first example, we compare SOCOL with CALIPSO along a single flight track. Figure 3 shows a curtain of observed ~~backscatter ratios~~ inverse backscatter ratios $1/R_{532}$ along orbit 2 on ~~01~~ 1 July 2007 (Fig. 3a) and the corresponding PSC

compositions (Fig. 3gd). The observations ~~show~~ indicate a large PSC over the Antarctic Peninsula (~~300E~~270 - ~~270~~300°E), and a smaller PSC over Oates Land (~~190E~~160 - ~~160~~190°E). Further, some tropospheric cirrus clouds were classified as PSCs. Above the Antarctic Peninsula, two distinctive regions with very small $1/R_{532}$ values ~~above 50~~ are evident. These high backscatter ratios ($R_{532} > 50$) are related to high number densities of ice particles (up to 10 cm^{-3}, Hu et al., 2002), which are caused by rapid cooling rates associated with mountain wave events. These wave ice clouds are surrounded by more synoptic scale PSCs with lower R_{532} values, which are classified as ice, STS and NAT mixtures.

Figures 3b and 3d show the corresponding plots for the PSCs as simulated by the SOCOL model in the respective grid boxes overflown by CALIPSO. Figures 3c and 3f show the same, but before detection thresholds and instrument uncertainty had been added. The model output also reveals a large PSC over the Antarctic Peninsula. However, the spatial extent of the simulated PSC is larger. The simulated backscatter ratio R_{532} peaks around 6, which is substantially lower than observed. Due to the coarse resolution and ~~orography~~the rather smooth orography in the model, SOCOL is not able to capture high ice particle number densities associated with small-scale mountain wave events. Applying the ~~CALIPSO~~ CALIOP classification scheme on the model output results in a layer of ice PSCs located around ~20 km, which is slightly higher than in the observations. The ice cloud is surrounded by NAT mixtures, while the observations indicate STS. Below those NAT mixtures, pure STS clouds occur in the model (Fig. 3f), most of which are tenuous enough such that they fully disappear after applying the optical thresholds (Fig. 3e).

The actual modeled composition (~~see Appendix,~~ Fig. A1) shows a similar pattern than the ~~CALIPSO~~ CALIOP classification scheme, but with more ice Mix and less STS. ~~These differences~~ This difference between actual composition and the composition according to the CALIPSO classification scheme of SOCOL PSCs can also be seen in Fig. 2c, where most of the ice mixtures (blue) are located in the NAT-Mix domain, while many NAT mixtures (green) are located in the STS domain. It should be noted that the modeled optical properties are exclusively calculated for PSCs. Tropospheric cirrus clouds treated by the model's cloud routine are therefore excluded.

3.2 Spatial distribution

Figure 4 presents monthly mean (including clear-sky and cloudy-sky conditions) backscatter ratios R_{532} from observations and simulation for July (a and b) and August 2007 (c and d). For a better comparison, the high-resolution measurements have been gridded onto the SOCOL grid. The data are vertically averaged over all pressure levels above the tropopause. The observations show a month-to-month variability in the location of the PSC region. In July~~2007~~, the mean backscatter intensity appears to be more homogeneously distributed, with a slight peak over East Antarctica (~0-150°E), while in August a distinct peak downstream of the Antarctic Peninsula (~55-70°W) is observed. This characteristic feature is caused by ~~the frequent mountain waves~~ frequent mountain wave events in this region (Hoffmann et al., 2017). These mountain waves lead to the formation of wave ice with very high backscatter values, but also to subsequent formation of enhanced NAT-mix clouds with high number densities of NAT particles (Zhu et al., 2017a).

The modeled month-to-month variability ~~of~~ in the R_{532} values and areal extent agrees well with CALIPSO observations. In July, the center of the PSC area is also tilted towards East Antarctica and slightly towards the Peninsula in August. However,

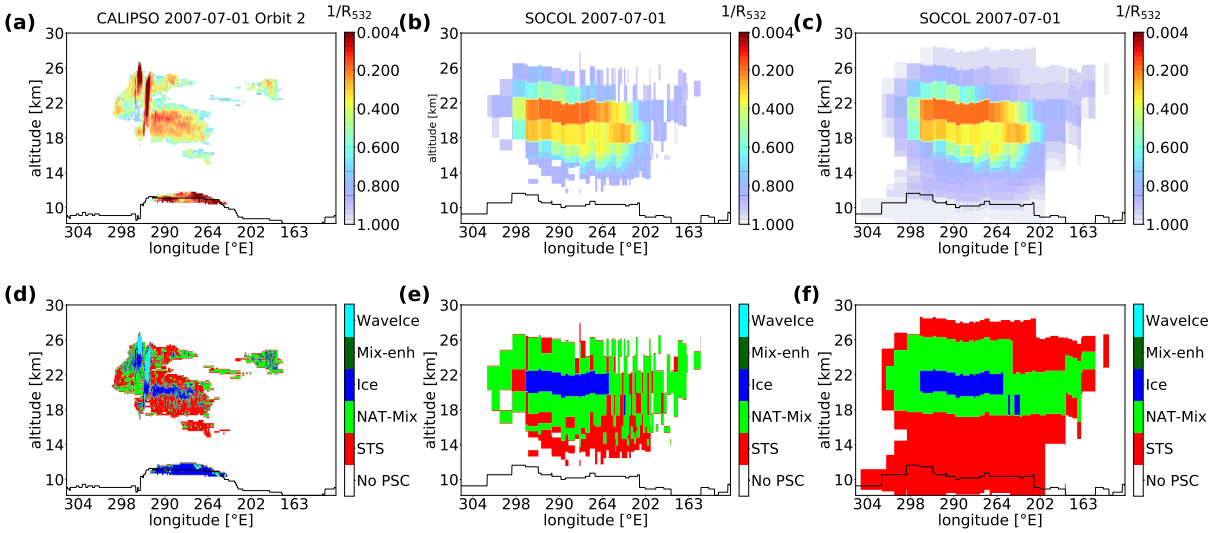

Figure 3. CALIPSO measurements on ~~01~~ 1 July 2007 (orbit 2) of R_{532} (a) and the PSC classification (d). ~~The calculated~~ Calculated R_{532} values ~~of~~ for modeled PSCs from the simulation S_{REF} in the overflown grid boxes after adding the instrument uncertainty and applying the detection thresholds are shown in (b). (e) shows the composition of the corresponding PSCs according to the classification scheme in Pitts et al. (2018). (c and f): The same as in (b and e), but without instrument uncertainty and the detection thresholds. The black lines indicate the WMO and model tropopause height for CALIPSO measurements and simulations, respectively.~~Note the different color scales for CALIPSO (a) and model backscatter (b and c).~~

peak values of R_{532} are clearly lower for SOCOL~~. In comparison to the observations, ~~, and the spatial distribution ~~of SOCOL PSCs~~ is more homogeneous. As mentioned above, this results mainly from a poor representation of mountain waves in the model~~.~~, but also from the fixed ice number density and upper limit for the NAT number density. Although the years 2006 and 2010 show a slightly different seasonal cycle (Fig. A5, A6), the conclusions on the model performance hold for those years as well.

3.3 PSC areal coverage

The total areal coverage as a function of altitude and time is a measure for the seasonal evolution of PSCs inside the polar vortex. Figure 5 compares CALIOP observations and model results for the winter 2007 (see also Fig. 13 in Pitts et al., 2018). The modeled PSC area is determined for every grid box based on the PSC occurrence for two output time steps per day, 0:00 and 12:00 UTC. We consider the entire model grid box to be covered by PSCs as soon as PSCs occur and exceed the detection limits. The observed PSC area is calculated in two different ways: (1) from the daily fraction of PSC measurements within ten equal-sized latitude bands ~~, while the~~ as described in Pitts et al. (2018) (Fig. 5a), and (2) from measurements average over 12 hours and gridded onto the SOCOL grid (Fig. 5b). The second method is similar to the calculation of the modeled PSC area ~~is determined for every grid box based on the PSC occurrence (above the detection thresholds) for two time steps per day.~~

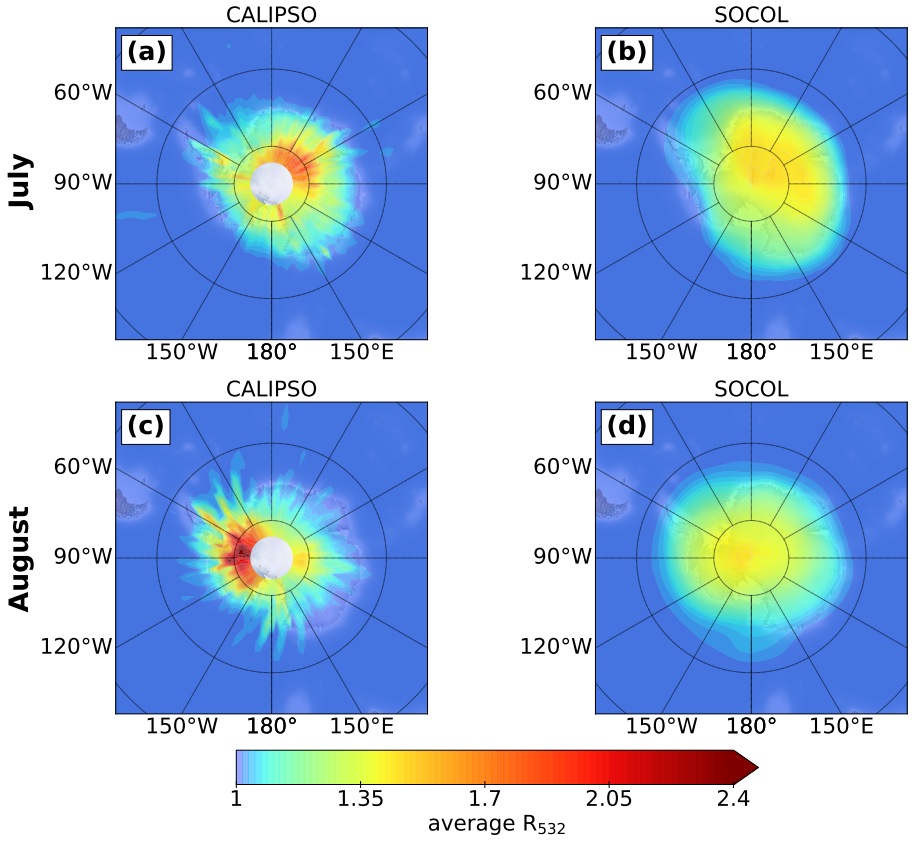

Figure 4. ~~Gridded (on SOCOL grid) and vertically~~ Vertically integrated monthly means of R_{532} for all-sky conditions as observed by CALIPSO (a and c, gridded onto the SOCOL grid) and as simulated by SOCOL from the simulation S_{REF} (b and d), for July (~~a and b~~top) and August 2007 (~~c and d~~bottom).

("SOCOL-method"). Since CALIOP does not over-pass all SOCOL grid cells within 12 hours, the "empty" grid cells are filled by the PSC area in the over-passed grid cells at the same latitude. We applied the "SOCOL-method" to the CALIOP data to achieve the best possible comparability between model and observations. Compared to Fig. 5a, the "SOCOL-method" leads to an increase in the CALIOP PSC areal coverage. Since CALIOP does not ~~measure~~ provide data poleward of 82°, measurements between ~~77.4~~ 77.8 and 82°S are assumed to be representative of the entire ~~77.4~~77.8–90°S latitude band.

Considering the low-level (11 - 12 km) clouds in May and June as tropospheric cirrus, the first PSC occurrence is observed in mid-May at 20-25 km altitude ~~.~~(Fig. 5a). Periods with higher PSC areal coverage with large vertical extent alternate with periods of less PSC extent. A clear peak occurs at end of July between 17 and 23 km altitude. The PSC areal coverage starts to decrease beginning of September, reaching zero mid-October. The descent of the coldest temperatures within the winter season is reflected in the descent of PSC occurrence. As described in Pitts et al. (2018), the PSCs merge with tropospheric cirrus clouds at mid-July.

In SOCOL, PSC formation starts about 2 weeks earlier ~~.~~ (Fig. 5c). The model is capable of reproducing the temporal occurrence of the individual peaks end of July. Also the overall descent of maximum PSC coverage is present in the simulation. ~~PSC~~ PSCs exist until end of October, which is longer than observed. ~~However~~Furthermore, SOCOL simulates a substantially larger PSC area than observed (Fig. 5a), in particular between 13 and 23 km altitude, where $1.5 \cdot 10^7$ km^2 are almost continuously exceeded.

~~It is most likely that the different methods for calculating PSC areal coverage contributes to this overestimation. For each output time step, we considered the entire grid box to be covered by PSCs as soon as PSCs (above the detection thresholds)occur in the model. Further, also a cold-temperature~~ There are two main reasons for the overestimated PSC area and for the longer PSC period in the model. Part of the overestimation can be explained by the calculation method, since even small amounts of PSCs within a large model grid cell contribute substantially to the PSC areal coverage. However, SOCOL still overestimates CALIPSO when applying the "SOCOL-method" to the observations (Fig. 5b). Most of the overestimation results from a cold temperature bias in the ~~model contributes to the larger PSC area.~~polar lower stratosphere, which is typically around 2 to 4 K. Offsetting this cold bias by +3 K in a sensitivity simulation results in a decrease in the simulated PSC areal coverage (Fig. 5e) and a clearly improved agreement with CALIOP observations (Fig. 5b).

The modeled PSC area calculated without the optical thresholds applied (Fig. 5~~e~~d and f) is significantly larger, especially below 13 km altitude, where large areas with STS clouds occur in the model (see also Fig. 3f). Those large-scale STS clouds are very tenuous ~~since they are~~ and filtered out by applying the conservative PSC detection threshold~~and hence do not play an important role in ozone chemistry. However, it~~ . The contribution of those STS clouds to SAD is negligible. However, the comparison highlights the crucial role of the detection thresholds ~~when comparing PSC areas~~for model-measurement intercomparisons. Due to this sensitivity to the applied methods, quantitative comparisons of the areal coverage must be interpreted with caution.

Observed and simulated PSC coverage for the years 2006 and 2010 are shown in Figs. A5 and A6. In 2006, the year with above-average PSC occurrence, offsetting the cold bias leads to a smaller PSC coverage than observed, indicating that not the synoptic-scale temperature, but rather small-scale temperature fluctuations determined the PSC occurrence and areal coverage in 2006 (see also Fig. A3). As such small-scale features are not adequately represented in SOCOL, correcting for the synoptic-scale temperature bias leads to an underestimation of the PSC coverage.

3.4 Sensitivity to microphysical parameters

As described in Sect. 2.1, SOCOL's PSC scheme includes some prescribed microphysical parameters such as the ice particle number density, n_{ice}, or the NAT radius, r_{NAT}. These values had once been chosen based on what was known about PSCs back then. However, the current parameter setting might not be optimal. For example, the rather low value for n_{ice} of 0.01 cm^{-3} prevents the formation of ice PSCs with high number densities as observed in mountain wave events. To investigate the sensitivity of the simulated PSCs to the ~~microphysical parameters in the PSC scheme~~parameter setting, we performed additional simulations ~~for the Antarctic winter 2007~~ with increased n_{ice} and/or increased $n_{NAT,max}$ (Table 1). In addition, we performed a

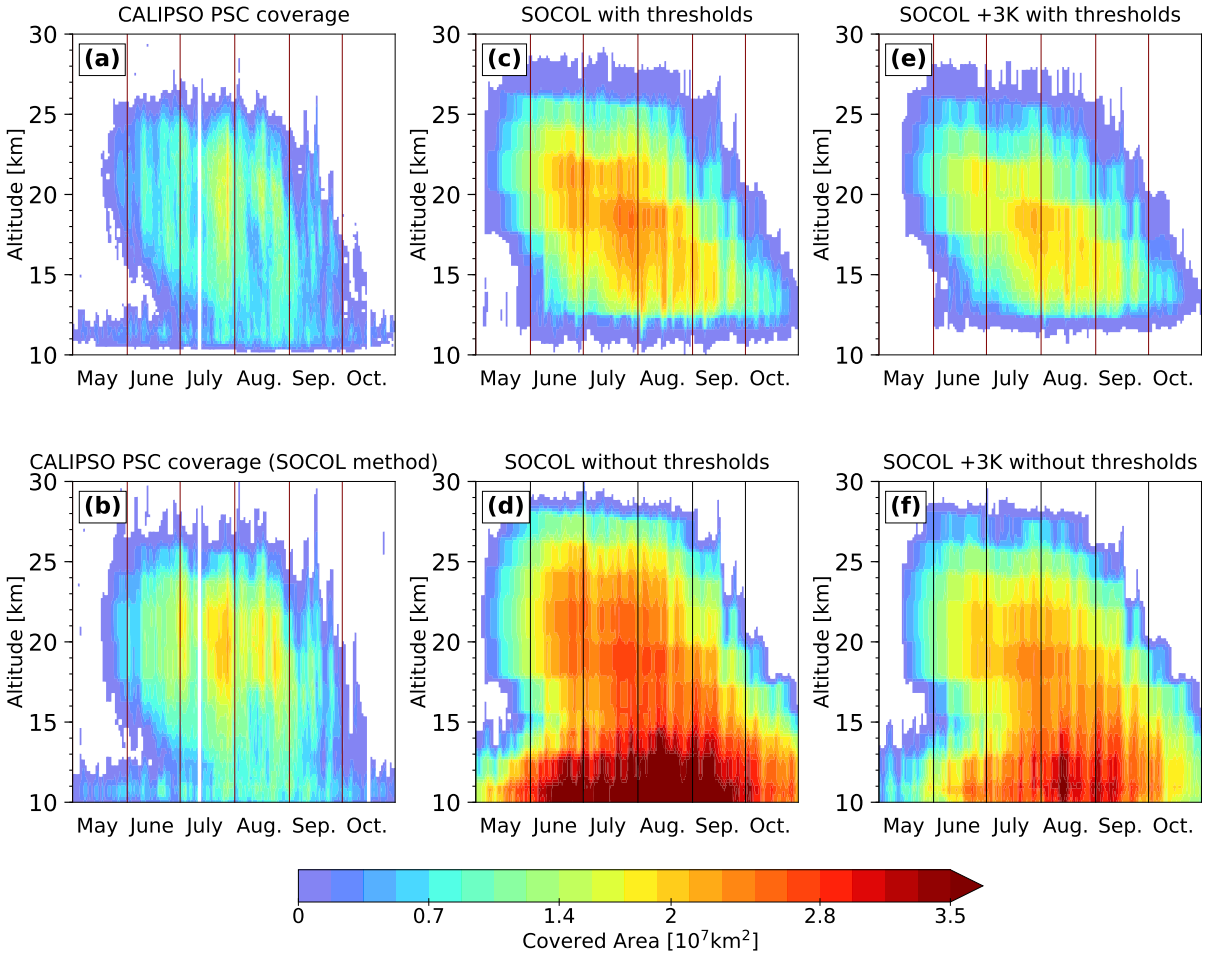

Figure 5. Time series of total PSC areal coverage over the Antarctic region as a function of altitude for the winter ~~2007~~ 2007. (a) derived from CALIOP as described in Pitts et al. (2018). (~~a~~b) ~~and simulated~~ derived from CALIOP by ~~SOCOL as it would have been detected by~~ applying the ~~CALIOP~~ "SOCOL-method" (~~b~~see text). (c) and (d): derived from the ~~simulated PSC areal coverage without applied optical thresholds~~ SOCOL reference simulation with and without ~~added~~ applying detection limits and instrument uncertainty, respectively. (e) and (f): same as for (c) and (d), but with PSC formation temperature increased by 3 K.

simulation with increased temperatures for PSC formation to investigate the effect of the cold temperature bias on simulated PSCs and chemical composition within the polar vortex.

355 Figure 6 shows the composite histograms for ~~the~~ various SOCOL simulations. There are considerable differences to the observations (Fig. 1), but also between the simulations. PSCs in the ~~REF simulation~~ reference simulation S_{REF} show a strong relative maximum located in the STS domain with $1/R_{532}$ values between 0.4 and 0.2 (Fig. 6a). Only very few PSCs are classified as ice, i.e. the relative maximum towards the upper right, as observed by CALIPSO, is missing. ~~That the PSC mixtures in the simulations are located more at the~~ The shift of modeled PSC towards the lower and left side of the histogram ~~can also~~

Table 1. Overview over the SOCOL simulations and the microphysical parameter settings.

Parameter	n_{ice}	$n_{\text{NAT,max}}$	r_{NAT}	$T_{PSC-formation}$
S_{REF}	0.01 cm^{-3}	5x10^{-4} cm^{-3}	5 μm	
$S_{n(ice)}$	**0.1 cm^{-3}**	5x10^{-4} cm^{-3}	5 μm	
$S_{n(NAT,max)}$	0.01 cm^{-3}	**2x10^{-3} cm^{-3}**	5 μm	
$S_{n(ice),n(NAT,max)}$	**0.05 cm^{-3}**	**1x10^{-3} cm^{-3}**	5 μm	
$S_{T,n(ice),n(NAT,max)}$	**0.05 cm^{-3}**	**1x10^{-3} cm^{-3}**	5 μm	+3 K

~~be seen~~ is also visible in Fig. 2c. There are several reasons for this difference~~.~~: First, SOCOL does not resolve small-scale mountain waves due to the coarse ~~model resolution and orography~~horizontal resolution and smooth orography applied in the model. Furthermore, the modeled PSCs are representative for large grid box (2.8°x2.8°horizontally and approximately 2 km vertically), while the observations resolve much smaller scale structures (starting from 5 km horizontally along a track and 180 m vertically). Finally, the fixed ice number density of 0.01 cm^{-3} ~~does~~ and upper limit for NAT number densities do not allow for large ice ~~particle~~ and NAT cross sections, even if mountain waves would be resolved. Based on these findings we performed one sensitivity simulation with a tenfold ice number density, $S_{n(ice)}$. As shown Fig. 6b the tenfold increase in n_{ice} results in a strong maximum ~~to~~ towards the upper right, mainly within the enhanced NAT mixture domain. The higher number density of ice particles increases the cross section of ice, leading to enhanced backscatter in ice-containing grid cells. Due to its solid state, backscatter from ice has δ_{aerosol}>0. This results in a shift towards higher R_{532} and higher δ_{aerosol} values in the histogram. Overall, modifying n_{ice} leads to a better agreement in optical properties with CALIPSO.

NAT PSCs play a twofold role in stratospheric ozone chemistry: Besides efficient halogen activation on their surfaces, the sedimentation of NAT particles leads to denitrification, which hinders deactivation of reactive halogens and facilitates catalytic ozone loss (Peter, 1997). While ice PSCs are less important for stratospheric ozone chemistry, NAT formation and subsequent denitrification of the stratosphere play a crucial role. NAT formation in SOCOL depends on two parameters, $n_{\text{NAT,max}}$ and r_{NAT}. To test the model's sensitivity to those parameters, we ran further simulations with the upper boundary for NAT number densities increased by a factor of four, $S_{n(NAT,max)}$, and the NAT radius increased from 5 to 7 µm. As both simulations showed similar changes, the latter is not presented here.

The simulation with four times higher $n_{\text{NAT,max}}$ (Fig. 6c) shows a maximum shifted towards lower R_{532} values compared to the REF simulation, which is located around the optical thresholds at the lower left corner. As long as temperatures are below T_{NAT} and enough HNO_3 is available for NAT formation, an increase in $n_{\text{NAT,max}}$ or r_{NAT} results in more HNO_3-uptake by NAT particles. This reduces the available gas-phase HNO_3 for STS growth. Also, more HNO_3 through sedimentation of the solid NAT particles is removed. With larger r_{NAT} this removal occurs even faster due to the higher sedimentation velocity. The reduction in surface area density of STS results in less backscatter and subsequently a shift towards lower R_{532} values in the composite histogram. This shift towards lower R_{532} values worsens agreement with observations.

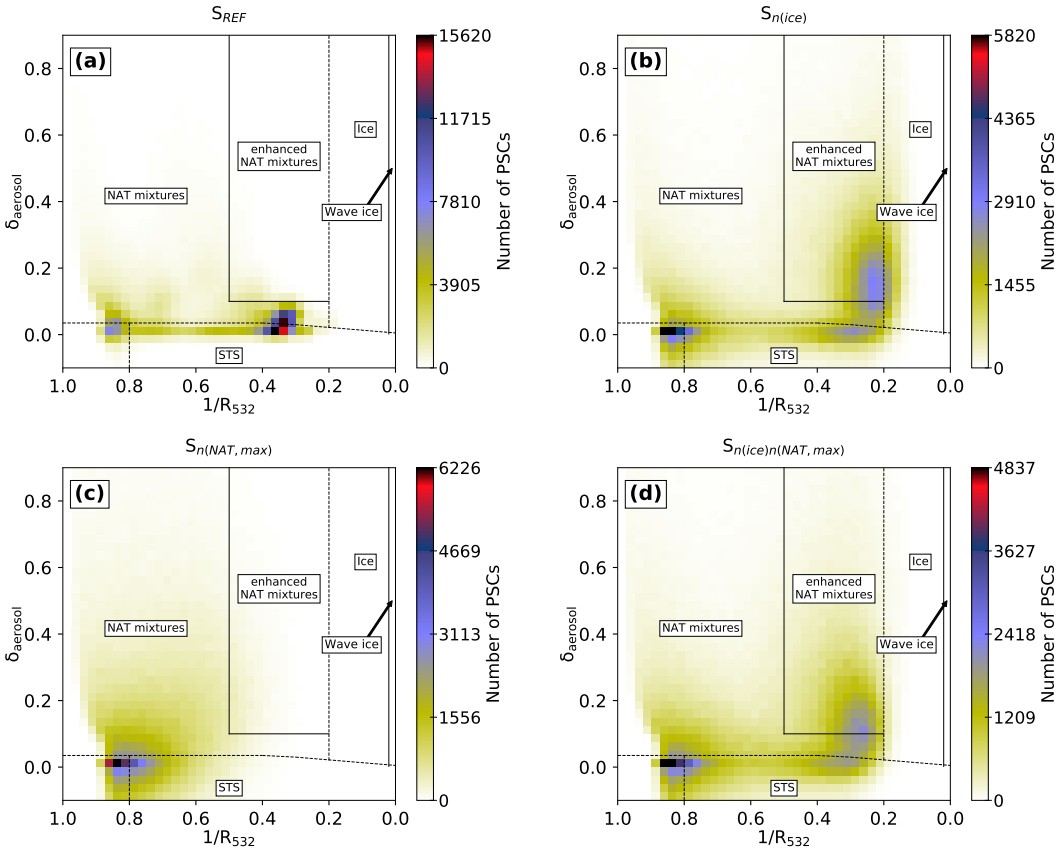

Figure 6. Composite 2D-histograms for July 2007, analogue to Fig. 1, for the simulations S_{REF} (a), $S_{n(ice)}$ (b), $S_{n(NAT,max)}$ (c) and $S_{n(ice),n(NAT,max)}$ (d).

In a ~~final~~ further simulation ($S_{n(ice),n(NAT,max)}$, Fig. 6d) we set n_{ice} to 0.05 cm^{-3} and $n_{\text{NAT,max}}$ to 10^{-3} cm^{-3}. This simulation shows a superposition of the two effects described above, resulting in two distinct relative maxima in the composite histogram. One maxima is located to the upper right, similar to $S_{n(ice)}$. The second maximum at low R_{532} and low δ_{aerosol} values is similar to the pattern in $S_{n(NAT,max)}$. The shift towards lower R_{532} values is again a result of less STS formation due to the reduced availability of HNO_3. Although the composition histograms of all sensitivity simulations still differ substantially from the observations, we find the best agreement for the simulation $S_{n(ice),n(NAT,max)}$. Similar shifts in the composite plots between the various model simulations as discussed above can be found for 2006 and 2010 (Figs. A7 and A8). In the model simulation $S_{T,n(ice),n(NAT,max)}$ including a cold bias correction of +3 K (Fig. A2) the synoptic-scale temperatures are too warm for substantial ice formation, emphasizing the importance of small-scale temperature fluctuations for ice PSCs.

To investigate the impact of the applied modifications on the simulated chemical composition of the polar stratosphere (60–82°S), we compare modeled gas-phase HNO_3, H_2O and O_3 with MLS measurements for 46 and 68 hPa (Figs. 7 - 9). To account for the spatial heterogeneity of the MLS measurements, we ~~calculated area-weighted concentrations for the~~ first

averaged the measurements over the SOCOL grid boxes. Afterwards we calculated area-weighted polar mean concentrations. The top panels shows absolute values for MLS ~~the REF~~ and the S_{REF} simulation, while the lower panels show the temporal evolution ~~relative to 01~~ for MLS and all model simulations relative to 1 May.

At the beginning of winter, all simulations have similar HNO_3 concentrations, which are about 20% to ~~100~~50% lower than MLS, depending on the pressure level ~~.~~(Fig. 7). At 46 hPa MLS HNO_3 starts to decline around mid-May and in early June at 68 hPa. Prior to the decline, an increase in HNO_3 is observed at 68 hPa. ~~It~~ This results from the evaporation of sedimenting NAT particles formed at higher altitudes (renitrification) and is an indication of denitrification of the upper levels. During July/August the absolute HNO_3 values from the reference run S_{REF} agree well with the observations. However, in late winter SOCOL again underestimates HNO_3 compared to MLS. All simulations show a decline due to HNO_3-uptake into NAT particles and STS droplets. However, S_{REF} (~~black~~red) and $S_{n(ice)}$ (~~cyan~~dark-blue) show a weaker and delayed HNO_3 decline with a plateau in July/August.

In $S_{n(NAT,max)}$ (green) the decline at both levels is considerably stronger than in S_{REF} as well as in MLS. This is due to the enhanced uptake of HNO_3 into NAT particles and the subsequent removal by sedimentation. As a consequence also the renitrification at lower levels is clearly enhanced. Both indicates a more efficient denitrification than in S_{REF}.

The simulation $S_{n(ice),n(NAT,max)}$ (~~red~~magenta), in which $n_{\mathrm{NAT,max}}$ is twice as large as in S_{REF}, but only half of $S_{n(NAT,max)}$, falls in between the other simulations. The denitrification starts about half a month later than in $S_{n(NAT,max)}$. The HNO_3-uptake is reduced and subsequently HNO_3 stays longer in the gas-phase. However, in August HNO_3 concentrations reach about the same level as in $S_{n(NAT,max)}$. Simulations with enhanced r_{NAT} have similar effects (not shown).

In $S_{T,n(ice),n(NAT,max)}$ denitrification as well as renitrification are delayed by about half a month due to the later onset of PSC formation. However, towards the end of the winter, HNO_3 concentrations are almost the same in all model simulations.

Figure 8 shows the same as Fig. 7, but for H_2O. As for HNO_3, all simulations start with similar H_2O values in May, but underestimate MLS by 20% to 30%. At 46 hPa MLS H_2O starts to decline beginning of June. Rehydration of lower levels due to the evaporation of sedimenting ice particles is observed shortly after. At 68 hPa, MLS H_2O starts to decrease mid of June. All model simulations except for $S_{T,n(ice),n(NAT,max)}$ show a very similar temporal evolution of H_2O in the polar stratosphere and a very good agreement with MLS. In SOCOL the amount of ice is determined by the amount of available H_2O and temperatures. The smaller the chosen n_{ice}, the larger the ice particles and the stronger the dehydration due to faster sedimentation. S_{REF} and $S_{n(NAT,max)}$, the simulations with the lowest n_{ice} of 0.01 cm^{-3}, show the strongest dehydration and the earliest onset, while $S_{n(ice)}$ with $n_{\mathrm{ice}} = 0.1\ \mathrm{cm}^{-3}$ shows the smallest dehydration ~~.~~of the simulations without modified PSC formation temperature. With the cold bias correction of +3 K, almost no dehydration takes place due to lack of ice formation. Changes in polar vortex H_2O from modifying n_{ice} have an influence on the SAD of NAT and STS, with higher H_2O concentrations leading to larger NAT and STS SADs. However, this effect is small compared to the effects from modifying the NAT-related microphysical parameters, and therefore, not further discussed.

Finally, Fig. 9 presents simulated O_3 in the polar stratosphere compared to MLS. At the beginning of winter all model simulations are in very good agreement with MLS measurements. For both pressure levels, the simulations show an earlier and stronger decline in O_3 than observed by MLS. Also, the recovery of O_3 starts earlier, leading to slightly higher O_3

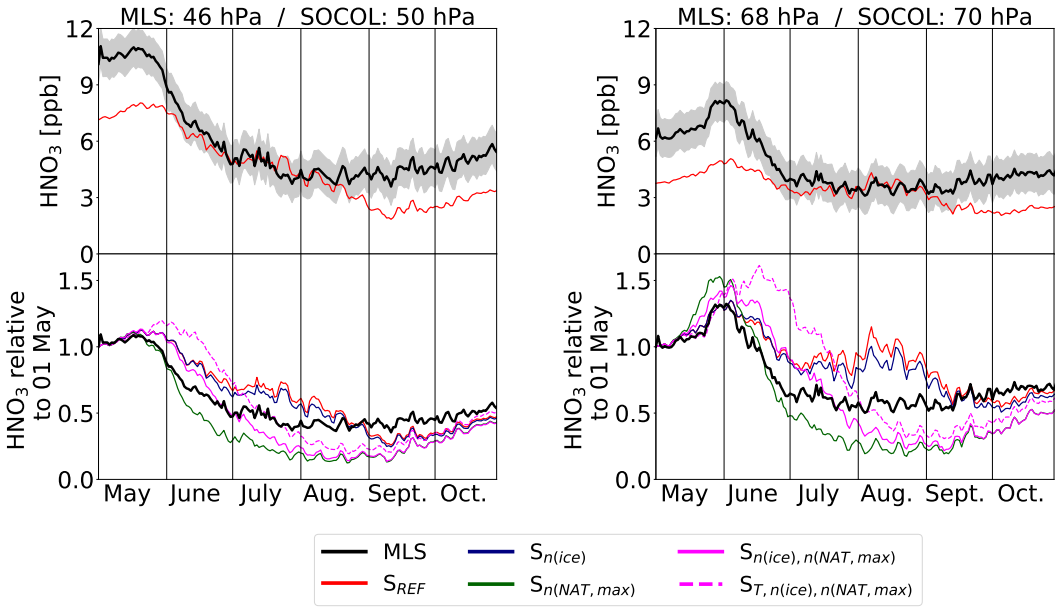

Figure 7. Temporal evolution of polar (60°S-82°S) mean gas-phase HNO_3 from MLS measurements and the different model simulations The uncertainty-range (gray shading) represent the MLS accuracy.

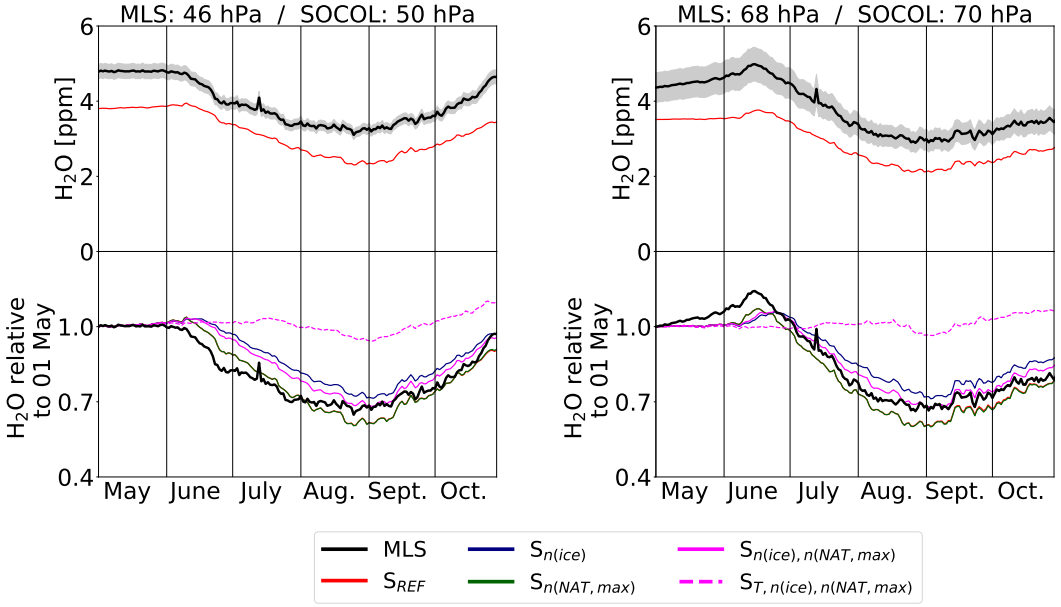

Figure 8. Same as Fig. 7, but for H_2O. Note that the line of $S_{n(NAT,max)}$ overlays S_{REF}, since these simulations have identical H_2O.

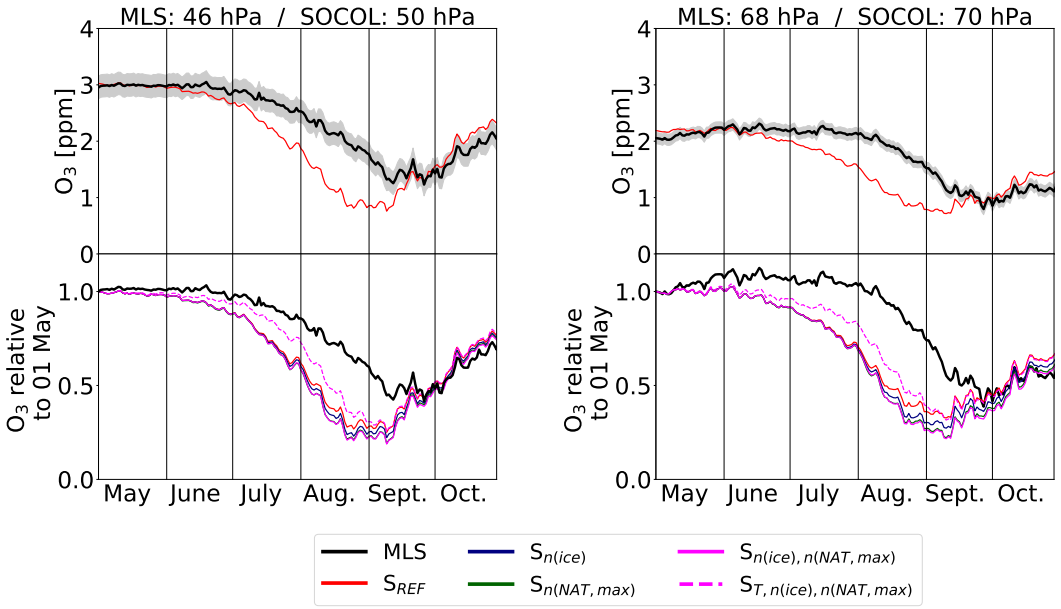

Figure 9. Same as Fig. 7, but for O_3.

values at the end of October. The spread among the model simulations is small compared to the differences to the observations, indicating minor effects of the PSC parameters on O_3-depletion. Increasing the parameter n_{ice} ~~affects the modeled stratospheric composition only very little by reducing dehydration. But~~ slightly reduces the simulated dehydration, but the increased SAD of ice leads to ~~slightly lower~~ a slightly stronger O_3 depletion in $S_{n(ice)}$ compared to S_{REF}. ~~Increasing the upper NAT boundary~~ Allowing for higher NAT number densities overall reduces SAD of ~~PSC~~ PSCs due to reducing the abundance of HNO_3. However, due to enhanced denitrification, $S_{n(NAT,max)}$ and $S_{n(ice),n(NAT,max)}$ show even slightly lower O_3 concentrations. O_3-depletion starts later in $S_{T,n(ice),n(NAT,max)}$ due to the later onset of PSC occurrence and smaller PSC area. However, from end of August onwards the differences between the individual model simulations vanish. The discussed findings for HNO_3, H_2O and O_3 hold also for the years 2006 and 2010, as shown in Figs. A11 to A14.

4 Discussion and Conclusions

~~We have~~ We presented an evaluation of ~~PSCs~~ polar stratospheric clouds (PSCs) in the Antarctic stratosphere as simulated by the ~~CCM~~ chemistry-climate model SOCOLv3.1~~in~~. The model was nudged towards ERA-Interim reanalysis (specified dynamics mode~~for the Antarctic winter 2007.~~). We compared modeled PSC occurrence and composition to CALIPSO/CALIOP satellite observations by mimicking a lidar measurement on the model output. The impact of PSCs on the chemical composition of the polar stratosphere by denitrification, dehydration and ozone depletion was investigated by comparison with Aura/MLS

satellite data. We analysed three winters with different PSC occurrence: 2006 (above-average), 2007 (average) and 2010 (below-average).

SOCOL considers STS droplets as well as water ice and NAT particles. PSCs are parametrized in terms of temperature and partial pressures of HNO_3 and H_2O, assuming equilibrium conditions. NAT and ice PSCs form instantaneously without taking the history of the air mass and preexisting PSC distributions into account. This approach states a simplification, but is successfully applied in other models as well (e.g., Wegner et al., 2013).

The PSCs scheme includes several fixed microphysical parameters, namely the maximum NAT number density, NAT radius and ice number density. ~~PSC occurrence and composition have been compared to CALIPSO/CALIOP satellite observations by mimicking a lidar measurement on the model output. The impact of PSCs on the chemical composition of the polar stratosphere has been investigated by comparison with Aura/MLS data~~Fixing the NAT radius leads to a homogeneous sedimentation velocity for all NAT particles, but allows for varying NAT number densities. Other models choose the reverse approach with fixed number densities, which results in varying NAT radius and sedimentation velocities (e.g., Wegner et al., 2013; Nakajima et al., 2016). In reality, the actual value for the NAT number density is far from being constant, because the active sites for NAT nucleation themselves show a wide distribution of efficacies (Hoyle et al., 2013). Both approaches require some tuning of the microphysical parameters to reasonably simulate observed sedimentation and denitrification. This was done here by various sensitivity simulations.

Overall, the spatial distribution of modeled PSCs is in reasonable agreement with CALIOP observations~~is good and the~~, and the model captures the observed month-to-month variability~~is represented~~. However, due to the coarse model ~~,~~ resolution and mean orography, but also due to the fixed ice number densities ~~, mountain wave events and associated wave ice~~ and upper limit for NAT number densities, mountain-wave induced ice and enhanced NAT clouds with high backscatter ratios, mainly observed over the Antarctic Peninsula, are not resolved ~~in SOCOL . The temporal and spatial evolution of PSCs inside the polar vortex as expressed by the areal coverage indicates an~~ by the SOCOL model. The PSC areal coverage over Antarctica indicates a continuous overestimation of PSCs in SOCOL. ~~This is~~ As shown by a sensitivity simulation, this can be partly explained by ~~a~~ the simulated cold temperature bias ~~, but also by the coarse model resolution~~in the winter polar stratosphere, which prevails despite running the model in specified dynamics mode. Furthermore, it is a consequence of the large grid size: even a small amount of PSCs within a grid cell adds a large contribution to the areal coverage. ~~This is reflected by the sensitivity of this quantity towards the applied detection thresholds.~~

~~Furthermore, we have tested the assumptions about the maximum NAT number density, NAT radius and~~ The choice of the prescribed ice number density~~by various sensitivity simulations. The parameter~~ , n_{ice}, determines primarily the optical signal and dehydration of the polar vortex through its impact on the particle ~~cross section andalso dehydration due to changing settling velocitieswith changing particle radius~~size and, therefore, sedimentation velocities. While increasing n_{ice} from the original value of 0.01 cm^{-3} to 0.1 cm^{-3} improves the agreement of the optical signal with CALIOP measurements, the simulated dehydration is more realistic for smaller n_{ice} and~~therefore~~ , therefore, larger ice particles.

The upper ~~boundary~~ limit for NAT number densities determines the HNO_3-uptake and subsequently the ~~magnitude of~~ competition between simulated NAT and STS formation, which is crucial for halogen activation. ~~We have shown that for an~~

~~increased max.~~ Increasing the maximum NAT number densities improves the temporal agreement of de- and renitrification with MLS measurements~~is improved~~. However, SOCOL ~~in general~~ clearly underestimates observed HNO_3 in the polar stratosphere already before the PSC season, which makes a solid conclusion about the best set of microphysical parameters difficult. Despite stratospheric H_2O and in particular HNO_3 being very sensitive to changes in the microphysical parameters, we found the ~~microphysical parameter settings, the~~ impact on O_3 ~~is very small . Best~~ depletion to be surprisingly small.

Eliminating the cold temperature bias inside the polar vortex has a more pronounced impact on O_3 concentrations. The onset of O_3 depletion is delayed by one to two weeks. However, the maximum O_3 decline in September is overestimated by all model simulations compared the MLS. This suggests either a too strong heterogeneous ozone loss in the SOCOL model or shortcomings regarding the model's dynamics inside the polar vortex. The latter was discussed by Khosrawi et al. (2017) as potential reason for the underestimated polar vortex ozone concentrations in the EMAC chemistry-climate model. Brühl et al. (2007) found that, even in specified dynamics mode, the downward transport in the lower part of the polar vortex is too weak. Since the SOCOL model is based on the same general circulation model as EMAC, the underestimated polar stratospheric ozone concentrations in SOCOL are not necessarily exclusively caused by too strong chemical ozone destruction, but could also be related to a too weak downward transport, diminishing the re-supply with ozone-rich air masses from higher altitudes. This would explain why polar stratospheric ozone in the SOCOL model showed to be rather insensitive to modifications in the PSC scheme.

The co-existence of NAT and STS poses a substantial challenge to PSC parameterizations. As mentioned above, the SOCOL model addresses this issue by setting an upper limit for NAT number densities. Khosrawi et al. (2017, 2018) found underestimated PSC volume densities and denitrification/re-nitrification in the Arctic polar vortex simulated by the chemistry-climate model EMAC. The authors explained these findings with an unrealistic partitioning of gasphase HNO_3 into STS and NAT, with NAT forming first at the expense of STS, the main contributor to PSC volume density. In addition, the simulated NAT particles may be too small for significant gravitational settling and re-nitrification of lower atmospheric levels. Khosrawi et al. (2018) suggested an adjusted HNO_3 partitioning and/or an upper limit for NAT number densities, as applied in the SOCOL model, as one potential way to improve the model. A similar approach was implemented by Wegner et al. (2013) in the WACCM model. To account for the simultaneous occurrence of STS and NAT, they allow 20% of total available HNO_3 to form NAT at a supersaturation of 10, with a NAT number density of 10^{-2} cm^{-3}. This value is an order of magnitude larger than the upper limit applied in SOCOL. An even larger NAT number density of 10^{-1} cm^{-3} was used by Nakajima et al. (2016) in the ATLAS model. As Wegner et al. (2013), they allowed 20% of HNO_3 to go into NAT, while the rest is available for STS. These examples demonstrate that the best parameter setting for PSC schemes is strongly model dependent.

For the present study, we ran the model in a rather coarse resolution of T42L39. While higher resolutions are often discussed to improve the model performance, we do not expect any substantial drawbacks from the applied set-up. First, the model was used in specified dynamics mode, and we do not see major differences in modeled polar vortex temperatures or dynamics between a T42L39 and T42L90 simulation in nudged mode. Second, to capture mountain wave events, for example, we would need to go to very high horizontal resolutions, which are beyond the capabilities of current chemistry-climate models. This is supported by Khosrawi et al. (2017), who found only little differences in modeled polar stratospheric HNO_3 and O_3 between

a T42 and a T106 horizontal resolution. Even with an anticipated resolution of T255 (60 km or 0.54° at the equator) they would expect problems with the representation of small-scale temperature fluctuations due to mountain waves. To account for the effects of mountain-waves on PSC formation Orr et al. (2015) implemented a parameterization of stratospheric temperature fluctuations into the global chemistry-climate configuration of the UK MetOffice Unified Model. They found an increase of up to 50% in PSC SAD over the Antarctic peninsula during early winter. Despite the fact that the SOCOL model experiences a cold temperature bias in the polar winter stratosphere, the Antarctic peninsula is indeed a region with relatively too little PSC occurrence in the model (Fig. 4). This underestimation is even more pronounced in our sensitivity runs with increased PSC formation temperature. In a very recent study Orr et al. (2020) showed that the additional mountain-wave induced cooling leads to enhanced NAT SAD throughout the winter and beginning of spring, resulting in intensified chlorine activation, especially during late winter/early spring. Interestingly, the effects of the parameterized mountain-wave cooling are not limited to the Antarctic peninsula, but involve the whole polar vortex. These findings emphasize the important role of ozone for atmospheric dynamics and the climate system.

In summary, we found the best overall agreement with the CALIOP and MLS measurements ~~is found for this case study~~ with the NAT and ice number concentrations increased from their default values to n_{ice} = 0.05 cm^{-3} and $n_{\text{NAT,max}}$ = $1{\cdot}10^{-3}$ cm^{-3}, respectively. Our findings hold for all analyzed Antarctic winters. Further work would be required to extend our findings to simulated PSCs in the Arctic~~or to other years. Nevertheless, this study demonstrates that also a simplified PSC scheme~~, which shows a more pronounced interannual variability than Antarctica. Our study confirms previous studies showing that also simplified PSC schemes based on equilibrium assumptions may achieve good approximations of fundamental properties of ~~polar stratospheric clouds needed in chemistry-climate models~~PSCs. However, the best parameter set-up is strongly model dependent. General model deficiencies like temperature biases or transport influence the parameter choice, and should be prioritized in future model development.

Code and data availability. Since the full SOCOLv3.1 code is based on ECHAM5, users must first sign the ECHAM5 license agreement before accessing the SOCOLv3.1 code (http://www.mpimet.mpg.de/en/science/models/license/, last access: 2020). Then the SOCOLv3.1 code is freely available. The contact information for the full SOCOLv3.1 code as well as the source code of the PSC module and the Mie and T-matrix scattering code are available at http://doi.org/10.5281/zenodo.4094663. The simulation data presented in this paper can be downloaded from the ETH Research Collection via http://dx.doi.org/10.3929/ethz-b-000406548. CALIPSO lidar level 2 polar stratospheric cloud mask version 2.0 (v2) is available on request to Michael C. Pitts. MLS HNO_3, H_2O and O_3 data products have been downloaded from https://mls.jpl.nasa.gov/index-eos-mls.php (latest access 1.11.2018).

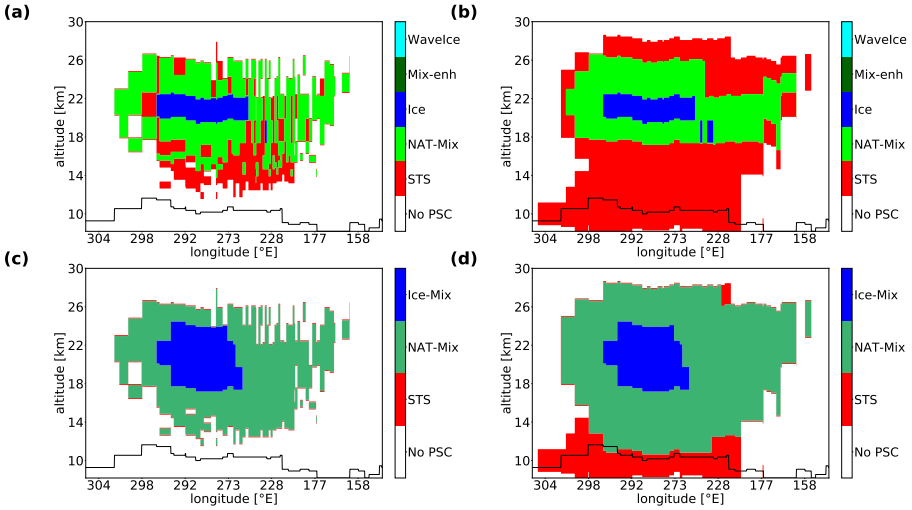

Figure A1. ~~Panels a) and b) show the composition according to the classification scheme in Pitts et al. (2018)~~ Composition of ~~the modeled~~ simulated PSCs ~~for~~ along the CALIPSO orbit 2 on 1 st July 2007 ~~case in~~ according to the ~~CALIOP orbit~~ classification scheme from ~~Fig. 3~~Pitts et al. (2018) after (a) and before (b) applying detection limits and ~~e~~instrument uncertainty. Panels c) and d) show the modeled PSC ~~composition~~type (STS: STS occurrence only; NAT-Mix: NAT but no ice occurrence; Ice-Mix: ice occurrence).

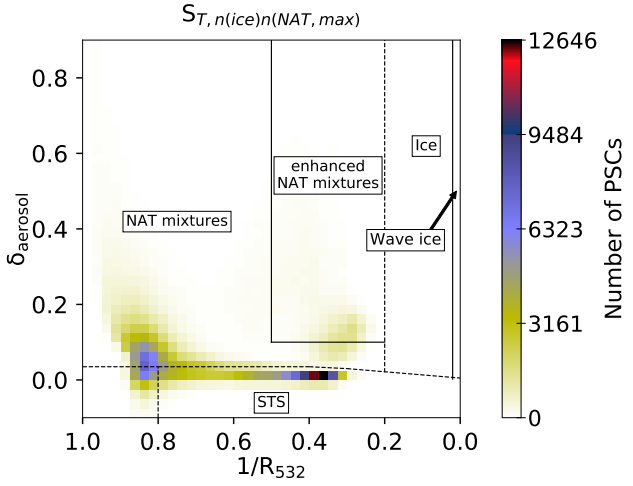

Figure A2. Composite 2D-histogram for July 2007, analogue to Fig. 1, for the simulation $S_{T,n(ice),n(NAT,max)}$.

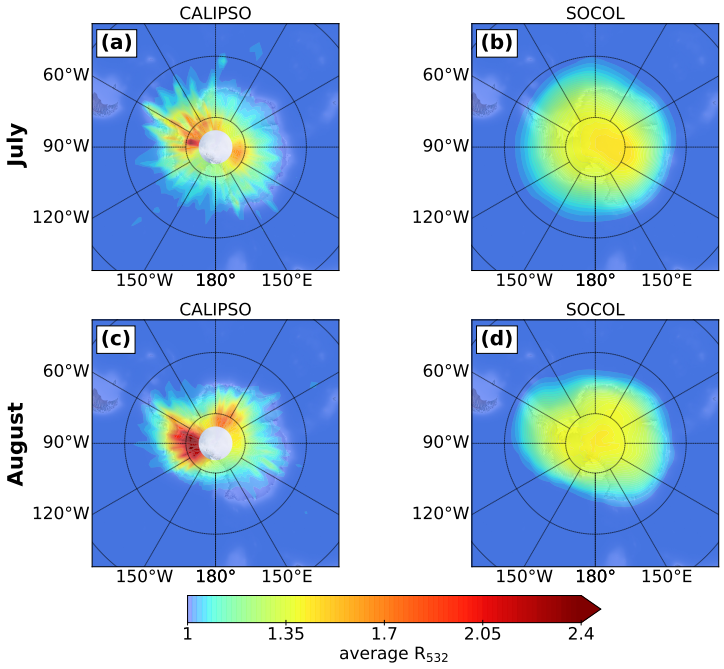

Figure A3. As Fig. 4, but for the year 2006.

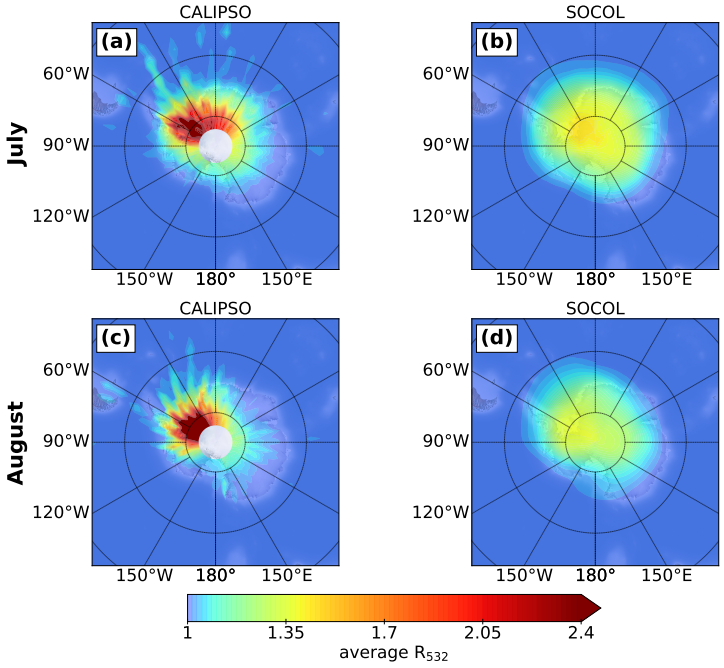

Figure A4. As Fig. 4, but for the year 2010.

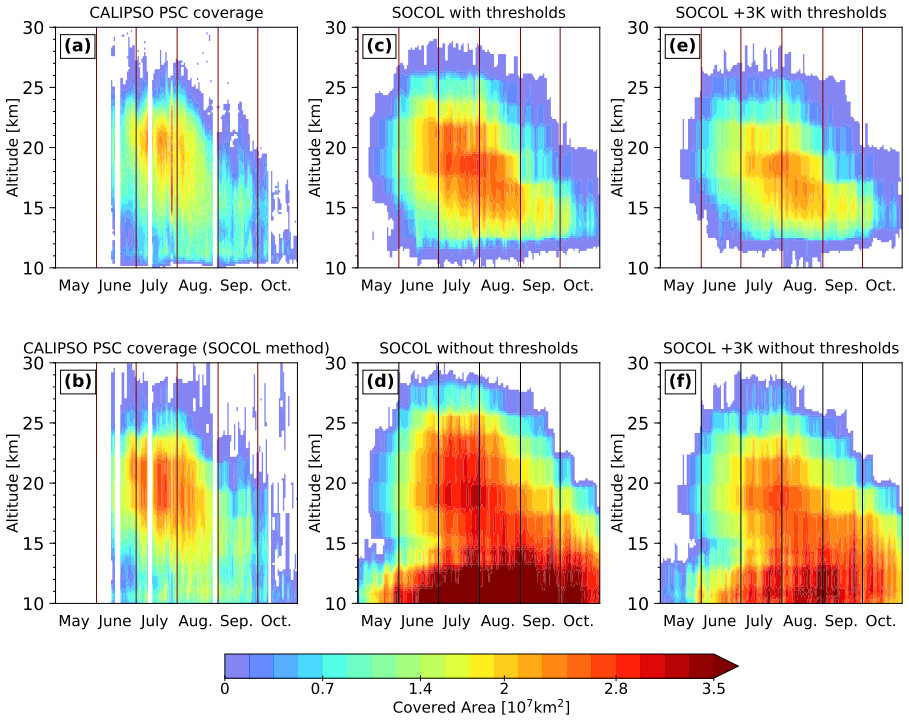

Figure A5. As Fig. 5, but for the year 2006.

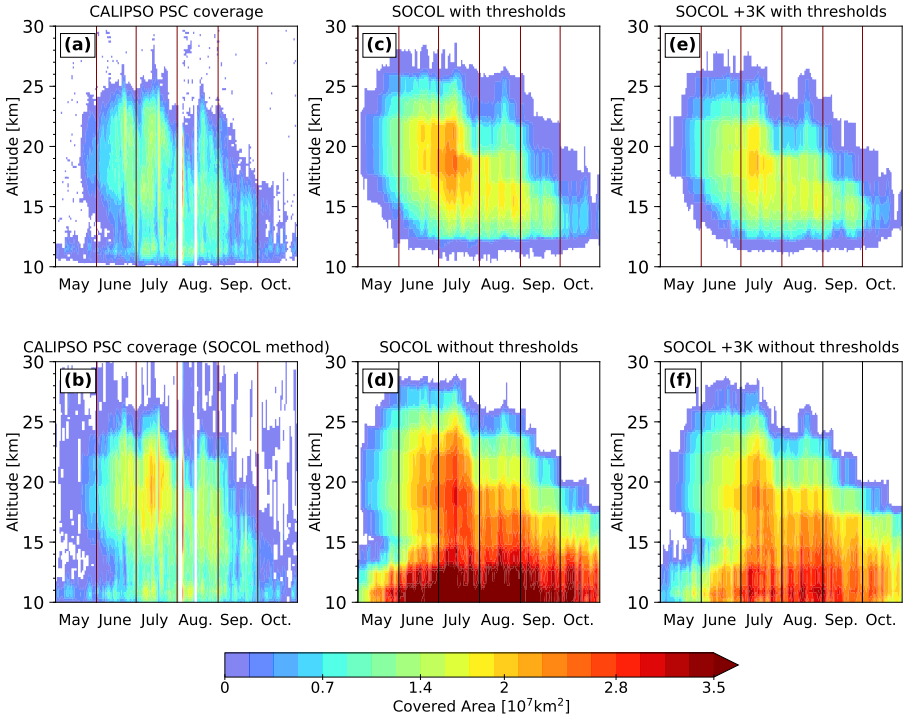

Figure A6. As Fig. 5, but for the year 2010.

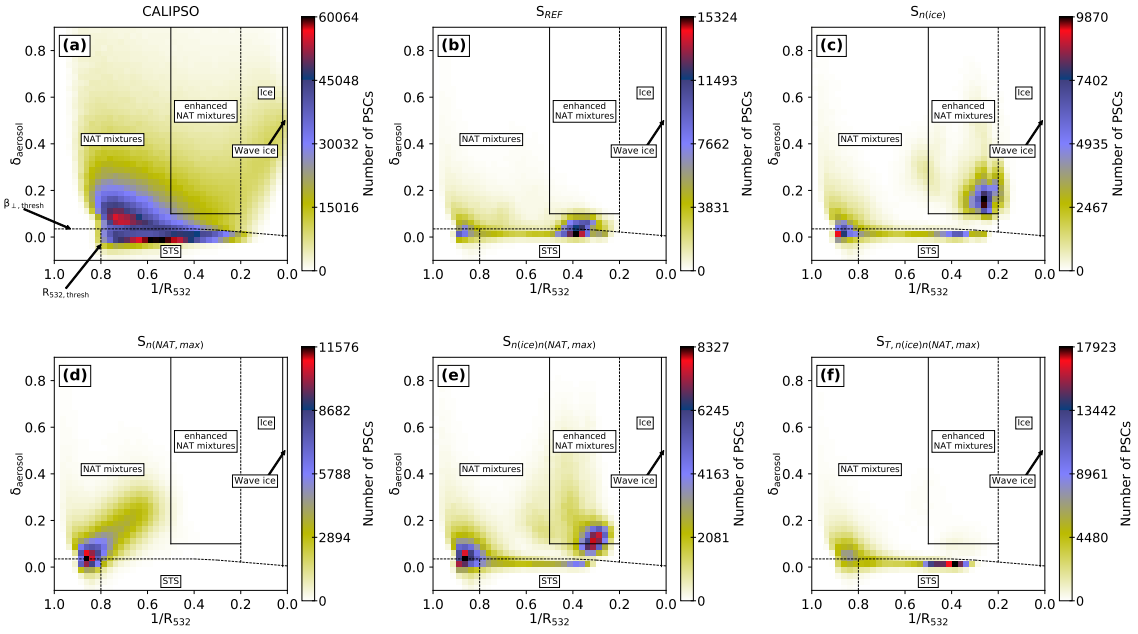

Figure A7. Composite 2D-histograms of CALIPSO measurements and SOCOL simulations as in Figs. 1, 6 and A2, but for the year 2006.

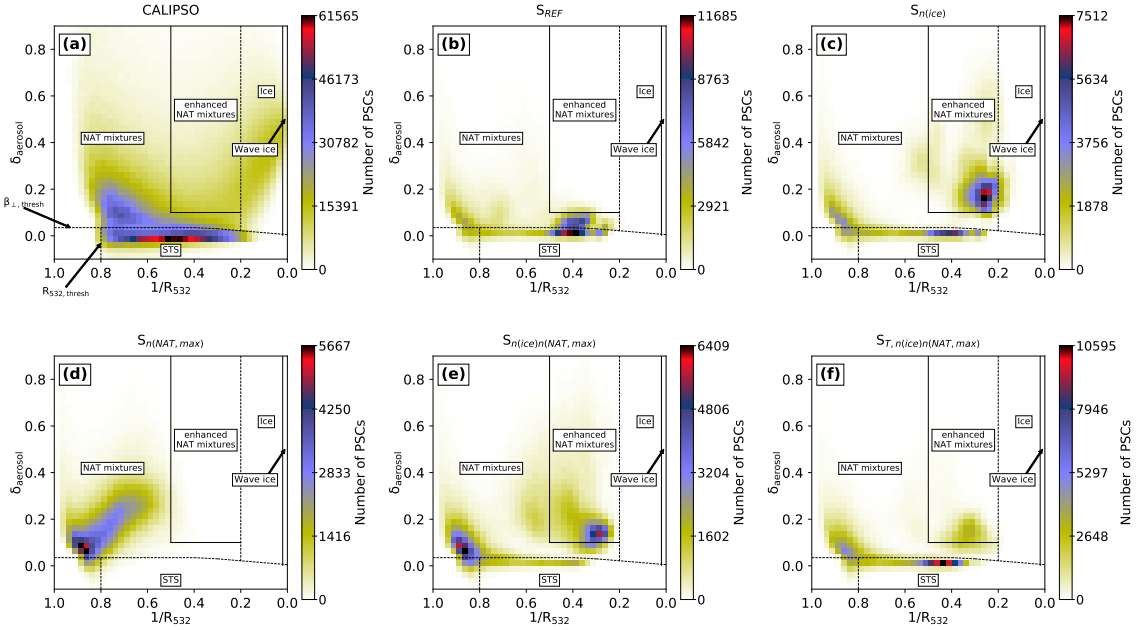

Figure A8. As Fig. A7, but for the year 2010.

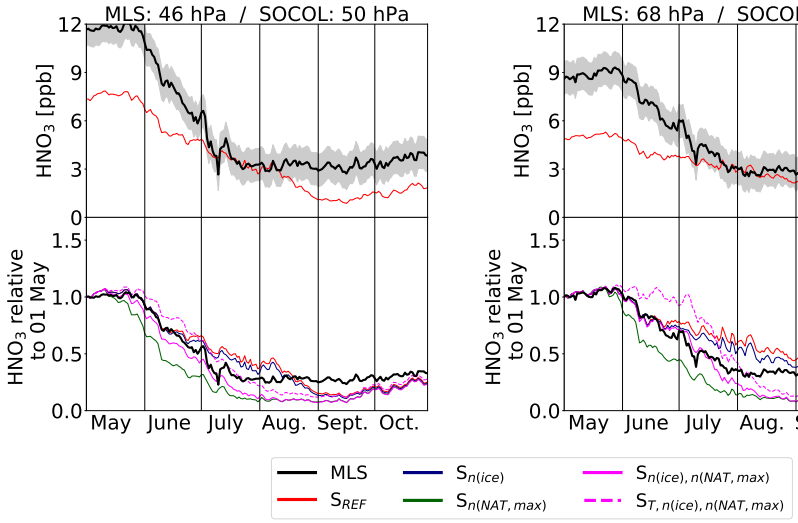

Figure A9. As Fig. 7, but for the year 2006.

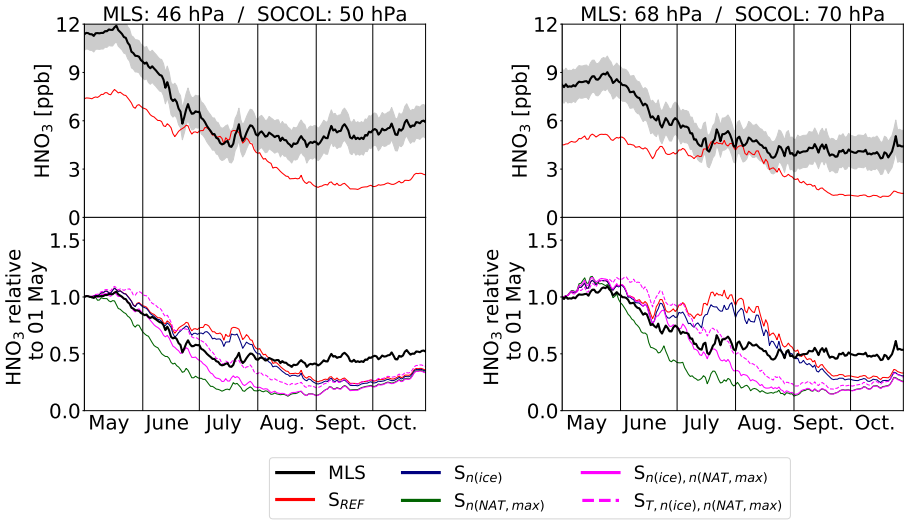

Figure A10. As Fig. 7 but for the year 2010.

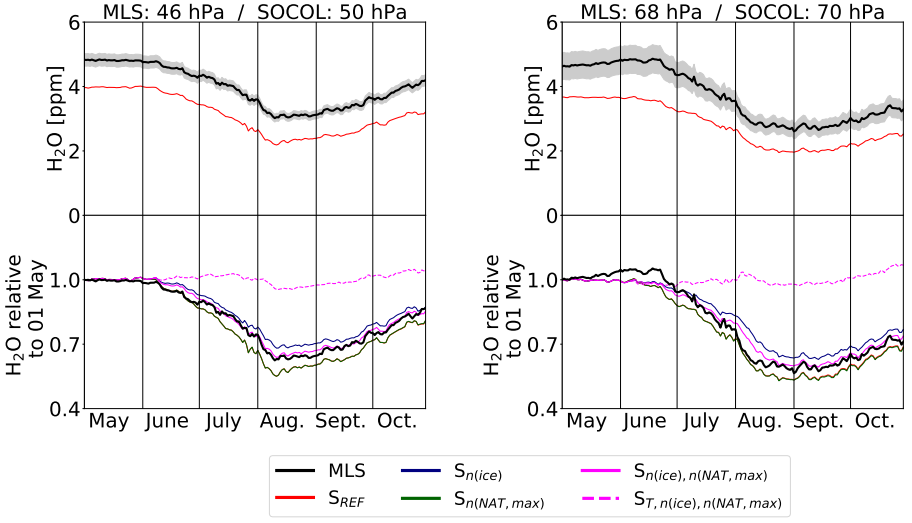

Figure A11. As Fig. 8, but for the year 2006.

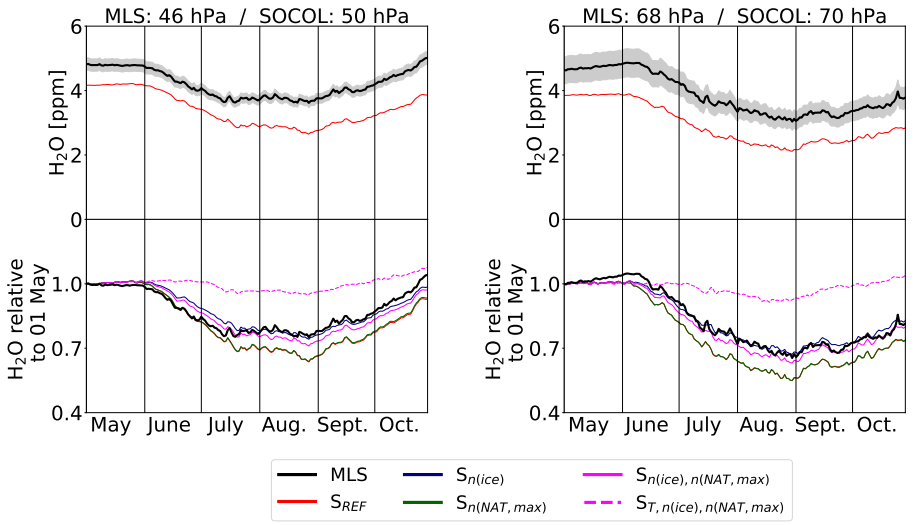

Figure A12. As Fig. 8, but for the year 2010.

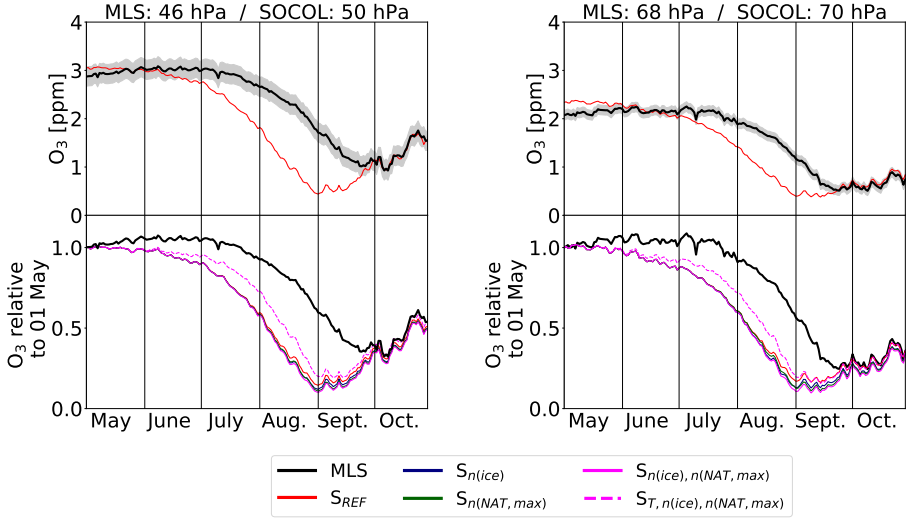

Figure A13. As Fig. 9, but for the year 2006.

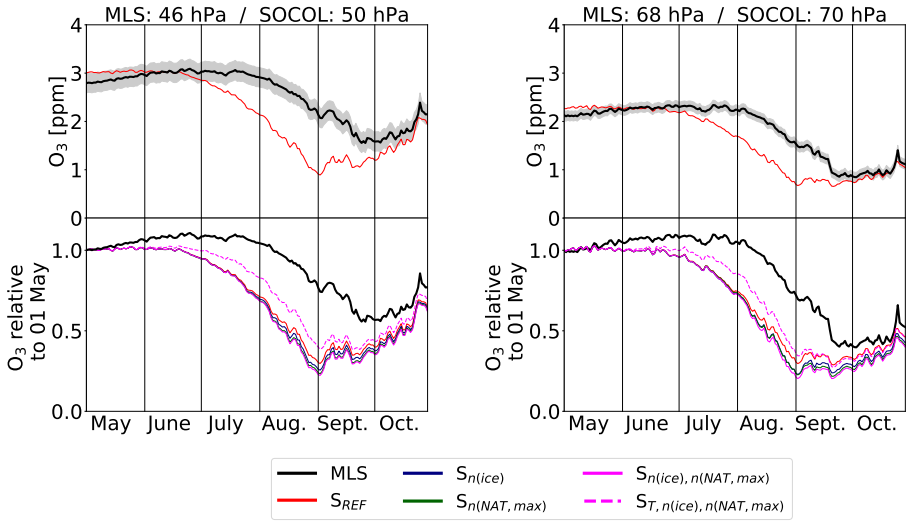

Figure A14. As Fig. 9, but for the year 2010.

Author contributions. AS and TP initiated the project of evaluating the PSC parametrization in SOCOL. AS conducted all SOCOL simulations. BL provided the Mie and T-matrix scattering code. MS analyzed the model results and wrote the paper. MP provided the CALIOP v2 data. All coauthors helped with the interpretation of the data and contributed to the manuscript.

Competing interests. The authors declare that they have no conflict of interest.

Acknowledgements. Special thanks go to Beiping Luo for providing the Mie and T-matrix scattering code. We thank Aryeh Feinberg and Franziska Zilker for their technical assistance and support. We also gratefully acknowledge Lamont Poole at NASA Langley Research Center for his help with the CALIPSO figures.

References

Akiyoshi, H., Zhou, L. B., Yamashita, Y., Sakamoto, K., Yoshiki, M., Nagashima, T., Takahashi, M., Kurokawa, J., Takigawa, M., and Imamura, T.: A CCM simulation of the breakup of the Antarctic polar vortex in the years 1980-2004 under the CCMVal scenarios, J. Geophys. Res., 114, https://doi.org/10.1029/2007jd009261, 2009.

Bardeen, C. G., Gettelman, A., Jensen, E. J., Heymsfield, A., Conley, A. J., Delanoe, J., Deng, M., and Toon, O. B.: Improved cirrus simulations in a general circulation model using CARMA sectional microphysics, J. Geophys. Res., 118, 11 679–11 697, https://doi.org/10.1002/2013jd020193, 2013.

Biele, J., Tsias, A., Luo, B. P., Carslaw, K. S., Neuber, R., Beyerle, G., and Peter, T.: Nonequilibrium coexistence of solid and liquid particles in Arctic stratospheric clouds, J. Geophys. Res., 106, 22 991–23 007, https://doi.org/10.1029/2001jd900188, 2001.

Brühl, C., Steil, B., Stiller, G., Funke, B., and Jöckel, P.: Nitrogen compounds and ozone in the stratosphere: comparison of MIPAS satellite data with the chemistry climate model ECHAM5/MESSy1, Atmospheric Chemistry and Physics, 7, 5585–5598, https://doi.org/10.5194/acp-7-5585-2007, https://acp.copernicus.org/articles/7/5585/2007/, 2007.

Carslaw, K. S., Luo, B. P., and Peter, T.: An analytic expression for the composition of aqueous $HNO_3-H_2SO_4$ stratospheric aerosols including gas-phase removal of HNO_3, Geophys. Res. Lett., 22, 1877–1880, https://doi.org/10.1029/95gl01668, 1995.

Daerden, F., Larsen, N., Chabrillat, S., Errera, Q., Bonjean, S., Fonteyn, D., Hoppel, K., and Fromm, M.: A 3D-CTM with detailed online PSC-microphysics: analysis of the Antarctic winter 2003 by comparison with satellite observations, Atmos. Chem. Phys., 7, 1755–1772, https://doi.org/10.5194/acp-7-1755-2007, 2007.

Dee, D. P., Uppala, S. M., Simmons, A. J., Berrisford, P., Poli, P., Kobayashi, S., Andrae, U., Balmaseda, M. A., Balsamo, G., Bauer, P., Bechtold, P., Beljaars, A. C. M., van de Berg, L., Bidlot, J., Bormann, N., Delsol, C., Dragani, R., Fuentes, M., Geer, A. J., Haimberger, L., Healy, S. B., Hersbach, H., Holm, E. V., Isaksen, L., Kallberg, P., Kohler, M., Matricardi, M., McNally, A. P., Monge-Sanz, B. M., Morcrette, J. J., Park, B. K., Peubey, C., de Rosnay, P., Tavolato, C., Thepaut, J. N., and Vitart, F.: The ERA-Interim reanalysis: configuration and performance of the data assimilation system, Q. J. R. Meteorol. Soc., 137, 553–597, https://doi.org/10.1002/qj.828, 2011.

Egorova, T. A., Rozanov, E. V., Zubov, V. A., and Karol, I. L.: Model for investigating ozone trends (MEZON), Izv. Atmos. Ocean. Phys., 39, 277–292, 2003.

Engel, I., Luo, B. P., Pitts, M. C., Poole, L. R., Hoyle, C. R., Grooß, J.-U., Dörnbrack, A., and Peter, T.: Heterogeneous formation of polar stratospheric clouds - Part 2: Nucleation of ice on synoptic scales, Atmos. Chem. Phys., 13, 10 769–10 785, https://doi.org/10.5194/acp-13-10769-2013, 2013.

Eyring, V., Bony, S., Meehl, G. A., Senior, C. A., Stevens, B., Stouffer, R. J., and Taylor, K. E.: Overview of the Coupled Model Intercomparison Project Phase 6 (CMIP6) experimental design and organization, Geoscientific Model Development, 9, 1937–1958, https://doi.org/10.5194/gmd-9-1937-2016, https://gmd.copernicus.org/articles/9/1937/2016/, 2016.

Fahey, D. W., Gao, R. S., Carslaw, K. S., Kettleborough, J., Popp, P. J., Northway, M. J., Holecek, J. C., Ciciora, S. C., McLaughlin, R. J., Thompson, T. L., Winkler, R. H., Baumgardner, D. G., Gandrud, B., Wennberg, P. O., Dhaniyala, S., McKinney, K., Peter, T., Salawitch, R. J., Bui, T. P., Elkins, J. W., Webster, C. R., Atlas, E. L., Jost, H., Wilson, J. C., Herman, R. L., Kleinböhl, A., and von König, M.: The detection of large HNO_3-containing particles in the winter arctic stratosphere, Science, 291, 1026–1031, https://doi.org/10.1126/science.1057265, 2001.

Farman, J. C., Gardiner, B. G., and Shanklin, J. D.: Large losses of total ozone in Antarctica reveal seasonal $ClOx/NOx$ interaction, Nature, 315, 207–210, https://doi.org/10.1038/315207a0, 1985.

Feng, W., Chipperfield, M. P., Davies, S., Mann, G. W., Carslaw, K. S., Dhomse, S., Harvey, L., Randall, C., and Santee, M. L.: Modelling the effect of denitrification on polar ozone depletion for Arctic winter 2004/2005, Atmos. Chem. Phys., 11, 6559–6573, https://doi.org/10.5194/acp-11-6559-2011, 2011.

Fischer, H. and Oelhaf, H.: Remote sensing of vertical profiles of atmospheric trace constituents with MIPAS limb-emission spectrometers, Appl. Opt., 35, 2787–2796, https://doi.org/10.1364/Ao.35.002787, 1996.

Fischer, H., Birk, M., Blom, C., Carli, B., Carlotti, M., von Clarmann, T., Delbouille, L., Dudhia, A., Ehhalt, D., Endemann, M., Flaud, J. M., Gessner, R., Kleinert, A., Koopman, R., Langen, J., Lopez-Puertas, M., Mosner, P., Nett, H., Oelhaf, H., Perron, G., Remedios, J., Ridolfi, M., Stiller, G., and Zander, R.: MIPAS: an instrument for atmospheric and climate research, Atmos. Chem. Phys., 8, 2151–2188, https://doi.org/10.5194/acp-8-2151-2008, 2008.

Garcia, R. R., Marsh, D. R., Kinnison, D. E., Boville, B. A., and Sassi, F.: Simulation of secular trends in the middle atmosphere, 1950-2003, J. Geophys. Res., 112, https://doi.org/10.1029/2006jd007485, 2007.

Garcia, R. R., Smith, A. K., Kinnison, D. E., de la Camara, A., and Murphy, D. J.: Modification of the Gravity Wave Parameterization in the Whole Atmosphere Community Climate Model: Motivation and Results, Journal of the Atmospheric Sciences, 74, 275–291, https://doi.org/10.1175/Jas-D-16-0104.1, <GotoISI>://WOS:000392419300016, 2017.

Gelaro, R., McCarty, W., Suarez, M. J., Todling, R., Molod, A., Takacs, L., Randles, C. A., Darmenov, A., Bosilovich, M. G., Reichle, R., Wargan, K., Coy, L., Cullather, R., Draper, C., Akella, S., Buchard, V., Conaty, A., da Silva, A. M., Gu, W., Kim, G. K., Koster, R., Lucchesi, R., Merkova, D., Nielsen, J. E., Partyka, G., Pawson, S., Putman, W., Rienecker, M., Schubert, S. D., Sienkiewicz, M., and Zhao, B.: The Modern-Era Retrospective Analysis for Research and Applications, Version 2 (MERRA-2), J. Clim., 30, 5419–5454, https://doi.org/10.1175/Jcli-D-16-0758.1, 2017.

Grooß, J.-U., Tritscher, I., and Chipperfield, M. P.: Polar Stratospheric Clouds in Global Models, in preparation, 2020.

Hanson, D. and Mauersberger, K.: Laboratory studies of the nitric-acid trihydrate - implications for the south polar stratosphere, Geophys. Res. Lett., 15, 855–858, https://doi.org/10.1029/GL015i008p00855, 1988.

Hoffmann, L., Spang, R., Orr, A., Alexander, M. J., Holt, L. A., and Stein, O.: A decadal satellite record of gravity wave activity in the lower stratosphere to study polar stratospheric cloud formation, Atmos. Chem. Phys., 17, 2901–2920, https://doi.org/10.5194/acp-17-2901-2017, 2017.

Höpfner, M., Larsen, N., Spang, R., Luo, B. P., Ma, J., Svendsen, S. H., Eckermann, S. D., Knudsen, B., Massoli, P., Cairo, F., Stiller, G., von Clarmann, T., and Fischer, H.: MIPAS detects Antarctic stratospheric belt of NAT PSCs caused by mountain waves, Atmos. Chem. Phys., 6, 1221–1230, https://doi.org/10.5194/acp-6-1221-2006, 2006.

Hostetler, C., Liu, Z., Reagan, J., Vaughan, M., Winker, D., Osborn, M., Hunt, W., Powell, K., and Trepte, C.: Calibration and Level 1 Data Products, https://www-calipso.larc.nasa.gov/resources/pdfs/PC-SCI-201v1.0.pdf, 2006.

Hoyle, C. R., Engel, I., Luo, B. P., Pitts, M. C., Poole, L. R., Grooß, J.-U., and Peter, T.: Heterogeneous formation of polar stratospheric clouds - Part 1: Nucleation of nitric acid trihydrate (NAT), Atmos. Chem. Phys., 13, 9577–9595, https://doi.org/10.5194/acp-13-9577-2013, 2013.

Hu, R. M., Carslaw, K. S., Hostetler, C., Poole, L. R., Luo, B. P., Peter, T., Fueglistaler, S., McGee, T. J., and Burris, J. F.: Microphysical properties of wave polar stratospheric clouds retrieved from lidar measurements during SOLVE/THESEO 2000, J. Geophys. Res., 107, https://doi.org/10.1029/2001jd001125, 2002.

Jiang, Y. B., Froidevaux, L., Lambert, A., Livesey, N. J., Read, W. G., Waters, J. W., Bojkov, B., Leblanc, T., McDermid, I. S., Godin-Beekmann, S., Filipiak, M. J., Harwood, R. S., Fuller, R. A., Daffer, W. H., Drouin, B. J., Cofield, R. E., Cuddy, D. T., Jarnot, R. F., Knosp, B. W., Perun, V. S., Schwartz, M. J., Snyder, W. V., Stek, P. C., Thurstans, R. P., Wagner, P. A., Allaart, M., Andersen, S. B.,

Bodeker, G., Calpini, B., Claude, H., Coetzee, G., Davies, J., De Backer, H., Dier, H., Fujiwara, M., Johnson, B., Kelder, H., Leme, N. P., Konig-Langlo, G., Kyro, E., Laneve, G., Fook, L. S., Merrill, J., Morris, G., Newchurch, M., Oltmans, S., Parrondos, M. C., Posny, F., Schmidlin, F., Skrivankova, P., Stubi, R., Tarasick, D., Thompson, A., Thouret, V., Viatte, P., Vömel, H., von der Gathen, P., Yela, M., and Zablocki, G.: Validation of Aura Microwave Limb Sounder ozone by ozonesonde and lidar measurements, J. Geophys. Res., 112, https://doi.org/10.1029/2007jd008776, 2007.

Jourdain, L., Bekki, S., Lott, F., and Lefevre, F.: The coupled chemistry-climate model LMDz-REPROBUS: description and evaluation of a transient simulation of the period 1980-1999, Ann. Geophys., 26, 1391–1413, https://doi.org/10.5194/angeo-26-1391-2008, 2008.

Khosrawi, F., Kirner, O., Sinnhuber, B.-M., Johansson, S., Höpfner, M., Santee, M. L., Froidevaux, L., Ungermann, J., Ruhnke, R., Woiwode, W., Oelhaf, H., and Braesicke, P.: Denitrification, dehydration and ozone loss during the 2015/2016 Arctic winter, Atmospheric Chemistry and Physics, 17, 12 893–12 910, https://doi.org/10.5194/acp-17-12893-2017, https://acp.copernicus.org/articles/17/12893/2017/, 2017.

Khosrawi, F., Kirner, O., Stiller, G., Höpfner, M., Santee, M. L., Kellmann, S., and Braesicke, P.: Comparison of ECHAM5/MESSy Atmospheric Chemistry (EMAC) simulations of the Arctic winter 2009/2010 and 2010/2011 with Envisat/MIPAS and Aura/MLS observations, Atmos. Chem. Phys., 18, 8873–8892, https://doi.org/10.5194/acp-18-8873-2018, 2018.

Kirner, O., Müller, R., Ruhnke, R., and Fischer, H.: Contribution of liquid, NAT and ice particles to chlorine activation and ozone depletion in Antarctic winter and spring, Atmos. Chem. Phys., 15, 2019–2030, https://doi.org/10.5194/acp-15-2019-2015, 2015.

Lambert, A., Read, W. G., Livesey, N. J., Santee, M. L., Manney, G. L., Froidevaux, L., Wu, D. L., Schwartz, M. J., Pumphrey, H. C., Jimenez, C., Nedoluha, G. E., Cofield, R. E., Cuddy, D. T., Daffer, W. H., Drouin, B. J., Fuller, R. A., Jarnot, R. F., Knosp, B. W., Pickett, H. M., Perun, V. S., Snyder, W. V., Stek, P. C., Thurstans, R. P., Wagner, P. A., Waters, J. W., Jucks, K. W., Toon, G. C., Stachnik, R. A., Bernath, P. F., Boone, C. D., Walker, K. A., Urban, J., Murtagh, D., Elkins, J. W., and Atlas, E.: Validation of the Aura Microwave Limb Sounder middle atmosphere water vapor and nitrous oxide measurements, J. Geophys. Res., 112, https://doi.org/10.1029/2007jd008724, 2007.

Livesey, N. J., Read, W. G., Wagner, P. A., Froidevaux, L., Lambert, A., Manney, G. L., Millán Valle, L. F., Pumphrey, H. C., Santee, M. L., Schwartz, M. J., Wang, S., Fuller, R. A., Jarnot, R. F., Knosp, B. W., Martinez, E., and Lay, R. R.: Earth Observing System (EOS), Aura Microwave Limb Sounder (MLS), Version 4.2 Level 2 data quality and description document, https://mls.jpl.nasa.gov/data/v4-2_data_quality_document.pdf, 2018.

Middlebrook, A. M., Berland, B. S., George, S. M., Tolbert, M. A., and Toon, O. B.: Real Refractive-Indexes of Infrared-Characterized Nitric-Acid Ice Films - Implications for Optical Measurements of Polar Stratospheric Clouds, Journal of Geophysical Research-Atmospheres, 99, 25 655–25 666, https://doi.org/Doi 10.1029/94jd02391, <GotoISI>://WOS:A1994PY22900026, 1994.

Mishchenko, M. I., Travis, L. D., and Mackowski, D. W.: T-Matrix computations of light scattering by nonspherical particles: A review, J. Quant. Spectrosc. Radiat. Transf., 55, 535–575, https://doi.org/10.1016/0022-4073(96)00002-7, 1996.

Molina, L. T. and Molina, M. J.: Production of Cl_2O_2 from the self-reaction of the ClO radical, J. Phys. Chem., 91, 433–436, https://doi.org/10.1021/j100286a035, 1987.

Morgenstern, O., Hegglin, M. I., Rozanov, E., O'Connor, F. M., Abraham, N. L., Akiyoshi, H., Archibald, A. T., Bekki, S., Butchart, N., Chipperfield, M. P., Deushi, M., Dhomse, S. S., Garcia, R. R., Hardiman, S. C., Horowitz, L. W., Jöckel, P., Josse, B., Kinnison, D., Lin, M. Y., Mancini, E., Manyin, M. E., Marchand, M., Marecal, V., Michou, M., Oman, L. D., Pitari, G., Plummer, D. A., Revell, L., Saint-Martin, D., Schofield, R., Stenke, A., Stone, K., Sudo, K., Tanaka, T. Y., Tilmes, S., Yamashita, Y., Yoshida, K., and Zeng, G.: Review of the global models used within phase 1 of the Chemistry-Climate Model Initiative (CCMI), Geosc. Model Dev., 10, 639–671, https://doi.org/10.5194/gmd-10-639-2017, 2017.

Nakajima, H., Wohltmann, I., Wegner, T., Takeda, M., Pitts, M. C., Poole, L. R., Lehmann, R., Santee, M. L., and Rex, M.: Polar stratospheric cloud evolution and chlorine activation measured by CALIPSO and MLS, and modeled by ATLAS.(Report)(Author abstract), Atmospheric Chemistry and Physics, 16, 3311, 2016.

Orr, A., Hosking, J. S., Hoffmann, L., Keeble, J., Dean, S. M., Roscoe, H. K., Abraham, N. L., Vosper, S., and Braesicke, P.: Inclusion of mountain-wave-induced cooling for the formation of PSCs over the Antarctic Peninsula in a chemistry–climate model, Atmospheric Chemistry and Physics, 15, 1071–1086, https://doi.org/10.5194/acp-15-1071-2015, https://acp.copernicus.org/articles/15/1071/2015/, 2015.

Orr, A., Hosking, J. S., Delon, A., Hoffmann, L., Spang, R., Moffat-Griffin, T., Keeble, J., Abraham, N. L., and Braesicke, P.: Polar stratospheric clouds initiated by mountain waves in a global chemistry–climate model: a missing piece in fully modelling polar stratospheric ozone depletion, Atmospheric Chemistry and Physics, 20, 12 483–12 497, https://doi.org/10.5194/acp-20-12483-2020, https://acp.copernicus.org/articles/20/12483/2020/, 2020.

Peter, T.: Microphysics and heterogeneous chemistry of polar stratospheric clouds, Ann. Rev. Phys. Chem., 48, 785–822, https://doi.org/10.1146/annurev.physchem.48.1.785, 1997.

Pitts, M. C., Poole, L. R., Dörnbrack, A., and Thomason, L. W.: The 2009-2010 Arctic polar stratospheric cloud season: a CALIPSO perspective, Atmos. Chem. Phys., 11, 2161–2177, https://doi.org/10.5194/acp-11-2161-2011, 2011.

Pitts, M. C., Poole, L. R., and Gonzalez, R.: Polar stratospheric cloud climatology based on CALIPSO spaceborne lidar measurements from 2006 to 2017, Atmos. Chem. Phys., 18, 10 881–10 913, https://doi.org/10.5194/acp-18-10881-2018, 2018.

Portmann, R., Solomon, S., Garcia, R., Thomason, L., Poole, L., and McCormick, M.: Role of aerosol variations in anthropogenic ozone depletion in the polar regions, Journal of Geophysical Research Atmospheres, 101, 22 991–23 006, 1996.

Pöschl, U., von Kuhlmann, R., Poisson, N., and Crutzen, P. J.: Development and intercomparison of condensed isoprene oxidation mechanisms for global atmospheric modeling, J. Atmos. Chem., 37, 29–52, https://doi.org/10.1023/A:1006391009798, 2000.

Pruppacher, H. R. and Klett, J. D.: Microphysics of clouds and precipitation, Springer, https://doi.org/10.1007/978-0-306-48100-0, 1997.

Read, W. G., Lambert, A., Bacmeister, J., Cofield, R. E., Christensen, L. E., Cuddy, D. T., Daffer, W. H., Drouin, B. J., Fetzer, E., Froidevaux, L., Fuller, R., Herman, R., Jarnot, R. F., Jiang, J. H., Jiang, Y. B., Kelly, K., Knosp, B. W., Kovalenko, L. J., Livesey, N. J., Liu, H. C., Manney, G. L., Pickett, H. M., Pumphrey, H. C., Rosenlof, K. H., Sabounchi, X., Santee, M. L., Schwartz, M. J., Snyder, W. V., Stek, P. C., Su, H., Takacs, L. L., Thurstans, R. P., Vömel, H., Wagner, P. A., Waters, J. W., Webster, C. R., Weinstock, E. M., and Wu, D. L.: Aura Microwave Limb Sounder upper tropospheric and lower stratospheric H_2O and relative humidity with respect to ice validation, J. Geophys. Res., 112, https://doi.org/10.1029/2007jd008752, 2007.

Revell, L. E., Tummon, F., Stenke, A., Sukhodolov, T., Coulon, A., Rozanov, E., Garny, H., Grewe, V., and Peter, T.: Drivers of the tropospheric ozone budget throughout the 21st century under the medium-high climate scenario RCP 6.0, Atmos. Chem. Phys., 15, 5887–5902, https://doi.org/10.5194/acp-15-5887-2015, 2015.

Roeckner, E., Brokopf, R., Esch, M., Giorgetta, M., Hagemann, S., Kornblueh, L., Manzini, E., Schlese, U., and Schulzweida, U.: Sensitivity of simulated climate to horizontal and vertical resolution in the ECHAM5 atmosphere model, J. Clim., 19, 3771–3791, https://doi.org/10.1175/Jcli3824.1, 2006.

Salawitch, R. J., Wofsy, S. C., Gottlieb, E. W., Lait, L. R., Newman, P. A., Schoeberl, M. R., Loewenstein, M., Podolske, J. R., Strahan, S. E., Proffitt, M. H., Webster, C. R., May, R. D., Fahey, D. W., Baumgardner, D., Dye, J. E., Wilson, J. C., Kelly, K. K., Elkins, J. W., Chan, K. R., and Anderson, J. G.: Chemical loss of ozone in the Arctic polar vortex in the winter of 1991-1992, Science, 261, 1146–1149, https://doi.org/10.1126/science.261.5125.1146, 1993.

Santee, M. L., Lambert, A., Read, W. G., Livesey, N. J., Cofield, R. E., Cuddy, D. T., Daffer, W. H., Drouin, B. J., Froidevaux, L., Fuller, R. A., Jarnot, R. F., Knosp, B. W., Manney, G. L., Perun, V. S., Snyder, W. V., Stek, P. C., Thurstans, R. P., Wagner, P. A., Waters, J. W., Muscari, G., de Zafra, R. L., Dibb, J. E., Fahey, D. W., Popp, P. J., Marcy, T. P., Jucks, K. W., Toon, G. C., Stachnik, R. A., Bernath, P. F., Boone, C. D., Walker, K. A., Urban, J., and Murtagh, D.: Validation of the Aura Microwave Limb Sounder HNO_3 measurements, J. Geophys. Res., 112, https://doi.org/10.1029/2007jd008721, 2007.

Schoeberl, M. R.: The EOS Aura Mission, pp. 64–70, Springer, New York, NY, https://doi.org/10.1007/978-0-387-35848-2_4, 2007.

Simpson, S., Chu, X., Liu, A., Robinson, W., Nott, G., Diettrich, J., Espy, P., and Shanklin, J.: Polar stratospheric clouds observed by a lidar at Rothera, Antarctica (67.5°S, 68.0°W), Proc. SPIE, 5887, https://doi.org/10.1117/12.620399, 2005.

Snels, M., Scoccione, A., Di Liberto, L., Colao, F., Pitts, M., Poole, L., Deshler, T., Cairo, F., Cagnazzo, C., and Fierli, F.: Comparison of Antarctic polar stratospheric cloud observations by ground-based and space-borne lidar and relevance for chemistry-climate models, Atmos. Chem. Phys., 19, 955–972, https://doi.org/10.5194/acp-19-955-2019, 2019.

Solomon, S., Garcia, R. R., Rowland, F. S., and Wuebbles, D. J.: On the depletion of Antarctic ozone, Nature, 321, 755–758, https://doi.org/10.1038/321755a0, 1986.

Stenke, A., Schraner, M., Rozanov, E., Egorova, T., Luo, B., and Peter, T.: The SOCOL version 3.0 chemistry-climate model: description, evaluation, and implications from an advanced transport algorithm, Geosc. Model Dev., 6, 1407–1427, https://doi.org/10.5194/gmd-6-1407-2013, 2013.

Tritscher, I., Grooß, J.-U., Spang, R., Pitts, M. C., Poole, L. R., Müller, R., and Riese, M.: Lagrangian simulation of ice particles and resulting dehydration in the polar winter stratosphere, Atmos. Chem. Phys., 19, 543–563, https://doi.org/10.5194/acp-19-543-2019, 2019.

Waters, J. W., Froidevaux, L., Harwood, R. S., Jarnot, R. F., Pickett, H. M., Read, W. G., Siegel, P. H., Cofield, R. E., Filipiak, M. J., Flower, D. A., Holden, J. R., Lau, G. K. K., Livesey, N. J., Manney, G. L., Pumphrey, H. C., Santee, M. L., Wu, D. L., Cuddy, D. T., Lay, R. R., Loo, M. S., Perun, V. S., Schwartz, M. J., Stek, P. C., Thurstans, R. P., Boyles, M. A., Chandra, K. M., Chavez, M. C., Chen, G. S., Chudasama, B. V., Dodge, R., Fuller, R. A., Girard, M. A., Jiang, J. H., Jiang, Y. B., Knosp, B. W., LaBelle, R. C., Lam, J. C., Lee, K. A., Miller, D., Oswald, J. E., Patel, N. C., Pukala, D. M., Quintero, O., Scaff, D. M., Van Snyder, W., Tope, M. C., Wagner, P. A., and Walch, M. J.: The Earth Observing System Microwave Limb Sounder (EOS MLS) on the Aura satellite, IEEE Trans. Geosci. Remote Sens., 44, 1075–1092, https://doi.org/10.1109/Tgrs.2006.873771, 2006.

Wegner, T., Grooss, J. U., von Hobe, M., Stroh, F., Suminska-Ebersoldt, O., Volk, C. M., Hosen, E., Mitev, V., Shur, G., and Muller, R.: Heterogeneous chlorine activation on stratospheric aerosols and clouds in the Arctic polar vortex, Atmospheric Chemistry and Physics, 12, 11 095–11 106, https://doi.org/10.5194/acp-12-11095-2012, <GotoISI>://WOS:000312411300030, 2012.

Wegner, T., Kinnison, D. E., Garcia, R. R., and Solomon, S.: Simulation of polar stratospheric clouds in the specified dynamics version of the whole atmosphere community climate model, J. Geophys. Res., 118, 4991–5002, https://doi.org/10.1002/jgrd.50415, 2013.

Winker, D. M. and Pelon, J.: The CALIPSO mission, in: IEEE International Geoscience and Remote Sensing Symposium. Proceedings, vol. 2, pp. 1329–1331, https://doi.org/10.1109/IGARSS.2003.1294098, 2003.

Winker, D. M., Hunt, W. H., and McGill, M. J.: Initial performance assessment of CALIOP, Geophys. Res. Lett., 34, https://doi.org/10.1029/2007gl030135, 2007.

Winker, D. M., Vaughan, M. A., Omar, A., Hu, Y. X., Powell, K. A., Liu, Z. Y., Hunt, W. H., and Young, S. A.: Overview of the CALIPSO Mission and CALIOP Data Processing Algorithms, J. Atmos. Oceanic Technol., 26, 2310–2323, https://doi.org/10.1175/2009jtecha1281.1, 2009.

Wohltmann, I., Lehmann, R., and Rex, M.: The Lagrangian chemistry and transport model ATLAS: simulation and validation of stratospheric chemistry and ozone loss in the winter 1999/2000, Geosc. Model Dev., 3, 585–601, https://doi.org/10.5194/gmd-3-585-2010, 2010.

Zhu, Y. Q., Toon, O. B., Lambert, A., Kinnison, D. E., Bardeen, C., and Pitts, M. C.: Development of a Polar Stratospheric Cloud Model Within the Community Earth System Model: Assessment of 2010 Antarctic Winter, Journal of Geophysical Research-Atmospheres, 122, 10 503–10 523, https://doi.org/10.1002/2017jd027003, <GotoISI>://WOS:000413675900022, 2017a.

Zhu, Y. Q., Toon, O. B., Pitts, M. C., Lambert, A., Bardeen, C., and Kinnison, D. E.: Comparing simulated PSC optical properties with CALIPSO observations during the 2010 Antarctic winter, J. Geophys. Res., 122, 1175–1202, https://doi.org/10.1002/2016jd025191, 2017b.